TÉCNICO LISBOA

一、人格完成に努むること

Confronting Multi-Higgs Models with Experiment

The Search for Underrated and Understudied Signals

Ricardo Miguel da Cunha Rosa Florentino

Thesis to obtain the Master of Science Degree in

Engineering Physics

Supervisors: Prof. João Paulo Ferreira da Silva
Prof. Jorge Manuel Rodrigues Crispim Romão

Examination Committee

Chairperson:	Prof. Mário João Martins Pimenta
Supervisor:	Prof. Jorge Manuel Rodrigues Crispim Romão
Member of the Committee:	Prof. Rui Alberto Serra Ribeiro dos Santos

October 2021

Dedicated to my mother

Acknowledgments

Firstly, I thank my supervisors, for without them, this work would not have come into fruition. Professor João Paulo Silva for accepting me as his pupil when I came to him, in my early university years, thirst for knowledge and work, and for his persistent quest to give me a noteworthy research topic. Professor Jorge Romão for his valuable insight in everything we discuss, and for the great work and effort he puts in everything he does.

I am grateful to my father for trusting all the decisions I make, supporting all the dreams I have and helping me to strive under all adversities. I thank my grandmother, my sisters and the rest of my family, for their constant presence and support.

To my friends David Fordham, Diogo Ivo and Pedro Piçarra, I am thankful for all the time we spent together and for always dreaming of me higher than I ever could. I thank Constança Freire for her unconditional support and motivation, Diogo Ribeiro for his most assertive friendship, and Patrícia Curado for being the energy and confidence I needed to conclude this journey.

I appreciate the learning experience and the work environment that the Physics Department of Instituto Superior Técnico provided me during these years. A special mention goes to Bruno Bento for the discussions of our work and to Francisco Vazão for sharing the experience of working under our supervisors. Likewise, I thank everyone at the Department of Physics of the Graduate School of Sciences of the University of Amsterdam for my year studding abroad.

Lastly, I bow to all karateka involved with the Estoril dojo for providing an open space for abstraction allowing me to focus on my self-improvement. I am forever indebted to my sensei Ivo Silva for his hand in preparing me for this challenge and all to come, and to Fernando Baptista for his eagerness to help me at all times.

This work has been partially supported by the *Fundação para a Ciência e Tecnologia* under the project LHC_CERN/FIS-PAR/0008/2019

Resumo

Estuda-se modelos Multi-Higgs que satisfazem simetria custodial, na procura de características fora do comum e pouco estudadas em sub-classes desses modelos. Ao estudar modelos com numero arbitrário de dubletos e singletos escalares, descobre-se que modelos com pelo menos dois dubletos e um singleto carregado têm a propriedade interessante de apresentar um acoplamento entre um bosão Z e dois escalares carregados de massas diferentes. Esta propriedade é normalmente ignorada em análises fenomenológicas, devido a estar ausente em modelos com apenas dubletos. Explora-se este problema em detalhe, considerando $h \to Z\gamma$, $B \to X_s\gamma$, e o decaimento de um escalar carregado pesado num mais leve e num bosão Z. Propõe-se que o ultimo seja procurado activamente no LHC, usando o sector escalar de Zee-type models como protótipo e propondo pontos de benchmark que obedeçam todos os dados experimentais correntes, e que possam estar no alcance do LHC.

Também se discute tópicos como o mecanismo de Higgs e a existência de carga, e como estes são influenciados numa teoria com simetrias de Gauge adicionais no sector electrofraco. Dá-se ênfase a teorias com grupo de Gauge eletrofraco $SU(2) \times U(1) \times U(1)$, e trabalha-se o exemplo de uma teoria com um dubleto e um multipleto maior.

Palavras-chave: Multi-Higgs; Zee Model; Gauge; LHC

Abstract

We study Multi-Higgs models which satisfy custodial symmetry in search of unusual and understudied characteristics in sub-classes of these models. Thus, we explore models with an arbitrary number of scalar doublets and singlets, finding that, within those, models containing at least two doublets and a charged singlet have the interesting property that they have couplings between one Z boson and two charged scalars of diferent masses. This property is often ignored in phenomenological analysis, as it is absent from models with only extra scalar doublets. We explore this issue in detail, considering $h \to Z\gamma$, $B \to X_s\gamma$, and the decay of a heavy charged scalar into a lighter one and a Z boson. We propose that the latter be actively searched for at the LHC, using the scalar sector of the Zee-type models as a prototype and proposing benchmark points which obey all current experimental data, and could be within reach of the LHC.

We also discuss the topics of the Higgs mechanism and the existence of charge, and how these are influenced in a theory with extra gauge symmetries in the electroweak sector, giving a particular emphasis to theories with an $SU(2) \times U(1) \times U(1)$ electroweak gauge group and working the example of one of those theories with a scalar doublet and a higher multiplet.

Keywords: Multi-Higgs; Zee Model; Gauge; LHC

Contents

List of Figures

List of Tables

Nomenclature

Roman symbols

$\mathrm{Im}(\ )$ Imaginary part.

$\mathcal{L}$ Lagrangian density.

$\mathrm{Re}(\ )$ Real part.

Superscripts

$*$ Complex conjugate; adimensional quantity

$\dagger$ Conjugate transpose (Hermitian conjugate).

T Transpose.

Acronyms

CERN Conseil Européen pour la Recherche Nucléaire.

DM Dark Matter.

LHC Large Hadron Collider.

SM Standard Model.

Chapter 1

Introduction

Over many decades, the Standard Model (SM) [1, 2, 3] has been confirmed to unprecedented precision. This culminated with the 2012 experimental detection of a fundamental scalar particle with mass 125GeV (the Higgs Boson h_{125}) [4, 5], which had been proposed in the early 1960's [6, 7]. Still, the SM leaves unanswered questions, from the nature of neutrino masses, to the origin of Dark Matter (DM). Having found one fundamental scalar, the most pressing question is: are there more fundamental scalars in Nature? There is a large international effort to answer this question, both from the theoretical point of view, and from the robust experimental physics programs currently pursued at CERN's LHC. Thus, one is lead to study and search for signals of extra scalars.

In Chapter 2 we give an introduction to concepts in Multi-Higgs physics in a pedagogical approach both to ease the reading of the rest of this work to the more inexperienced reader and to introduce the notations used later.

It is known experimentally that the masses of the W and Z bosons bear a relation very close to that predicted in the SM: $M_Z \cos\theta_W / M_W \sim 1$, where θ_W is the Weinberg angle. This holds automatically if the extra scalars are in doublets or singlets of the electroweak gauge group. Thus, we are lead to study theories with any number of scalar doublets and/or singlets; the latter neutral and/or charged.

In Chapter 3, starting with the Standard Model, we work our way up to introduce and study those models with an arbitrary number of doublets and singlets. We also go in more detail in one of those models, the Zee Model [8], consisting of two doublets and one charged singlet.

The Zee model is a case of particular interest, originally proposed to explain naturally small neutrino masses, and later adapted to explain also DM [9, 10]. The Zee model with an extra Z_2 symmetry proposed by Wolfenstein [11] is not consistent with current data from neutrino oscillations [12, 13], but the original proposal is still consistent with all leptonic experimental results [14, 15]. But the scalar sector of the Zee model (and of models having the same scalar sector, which we dub "Zee-type" models) also has another striking feature which is mostly ignored; it is the minimal model predicting the existence of couplings $Z H_1^{\pm} H_2^{\mp}$ between the Z gauge boson and two charged scalars (H_1^+ and H_2^+) of different mass.

This feature was the central motivation for a work which lead to the submission of an article for publication [16]. Along with part of Chapter 3, Chapter 4 was mainly adapted from this article.

Even before direct detection of the extra charged scalar particles, $ZH_1^{\pm}H_2^{\mp}$ couplings could potentially have a virtual effect on current measurements, such as $h_{125} \to Z\gamma$. We discuss this example in detail. In fact, the contribution of the charged scalars to the branching ratio can even vanish, but that is not because the Z couples to two different charged scalars, but rather because there are two charged scalars contributing in the loop. Indeed, this feature is already present for instance in the 3HDM, where there are two charged scalars but the coupling of the Z to them is diagonal. Although there is a modulation of the result with the mixing angle between the two charged Higgs, this is hidden when the sum over all diagrams is performed.

To study this model we took into account all the theoretical and experimental constraints coming from the scalar and quark sectors. In particular, we considered in detail the influence of the bounds coming from BR($B \to X_s\gamma$) [17]. This is especially important because, as there are two charged Higgs, one can evade the 580 GeV limit for the 2HDM [18]. We will discuss the implications of this for Zee-type models.

A distinctive signal for this model with its $ZH_1^{\pm}H_2^{\mp}$ couplings is the decay of the heavier charged Higgs into the lightest one and one Z. We performed an analysis of the parameter space to look for regions where this decay can be large. This lead us to identify examples of benchmark points where the decay $H_2^+ \to H_1^+ Z$ can be large as well as the decay $H_1^+ \to t\bar{b}$, leading to a clear signature that should be searched for at the LHC.

In Chapter 5 we study some of the concepts presented before but in the context of Multi-Higgs theories with larger Gauge groups in the electroweak sector. We also study a model with an $SU(2)_L \times U(1)_Y \times U(1)'$ symmetry and a scalar sector containing a doublet and a higher multiplet.

After the conclusions in Chapter 6, some appendices are included. In appendix A we collect the relevant couplings of the charged Higgs in Zee-type models. The detailed formulas for the loop decays are presented in appendix B and for perturbative unitarity in appendix C. As far as we know, the latter are presented in the submited article for the first time. Appendix D helps understand how the hypercharges change when we change the basis of the Gauge bosons, which is useful for Chapter 5.

Chapter 2

Concepts in Multi-Higgs Physics

In this chapter we introduce concepts the reader may be accustomed to see in the framework of the SM, but explored in a more broad context of general Multi-Higgs models. This will serve both as an invitation to broaden established concepts and as an introduction to the kind of notation used in this text. For practical purposes, in this chapter, we restrict ourselves to models invariant under the SM gauge group and omit the strong force group since it has no bearing in most of this work.

2.1 The Particle Content

Since our models are invariant under the electroweak gauge group of the SM, $SU(2)_L \times U(1)_Y$, all kinetic terms in the Lagrangian should use the covariant derivative

$$D_\mu \quad = \quad \partial_\mu + iK_\mu \,, \tag{2.1}$$

where

$$K_\mu = gT_a W_\mu^a + g'YB_\mu \,, \tag{2.2}$$

T_a are the $SU(2)$ generators and Y is the $U(1)$ hypercharge. These operators take different forms according to the fields the covariant derivative is acting on. By rotating the $SU(2)$ generators to a basis with a raising, a lowering and a diagonal operator, we can write K_μ as:

$$K_\mu = g(T_+ W_\mu^+ + T_- W_\mu^-) + gT_3 W_\mu^3 + g'YB_\mu \,. \tag{2.3}$$

where

$$W_\mu^\pm = \frac{W_\mu^1 \mp W_\mu^2}{\sqrt{2}} \tag{2.4}$$

and

$$T^{\pm} = \frac{T^1 \pm iT^2}{\sqrt{2}} \tag{2.5}$$

The $W_\mu^\pm$ are the charged carriers of the electroweak force, while W_μ^3 and B_μ will become the neutral carriers upon rotation to the mass eigenstates. As we will see later, this rotation depends on the content of the Higgs sector.

The fermionic sector is akin to the one of the SM. It includes three generations of particles, each with two $SU(2)$ doublets

$$Q_L = \begin{pmatrix} u_L \\ d_L \end{pmatrix} , \quad L_L = \begin{pmatrix} \nu_L \\ e_L \end{pmatrix} , \tag{2.6}$$

with hypercharges $1/6$ and $-1/2$ respectively, and three $SU(2)$ singlets

$$u_R , \quad d_R , \quad e_R , \tag{2.7}$$

with hypercharges $2/3$, $-1/3$ and -1 respectively. The $SU(2)$ generators act as the Pauli matrices on the doublets and as null operators on the singlets.

Finally, the Higgs sector will be restricted to an arbitrary number of doublets developing vevs in only the real part of one entry, so that, as we will see, electric charge remains unbroken. These can be expressed in the form

$$\Phi_i = \begin{pmatrix} \vdots \\ H_i^{++} \\ H_i^{+} \\ \frac{1}{\sqrt{2}}(v_i + h_i + ia_i) \\ \tilde{H}_i^{-} \\ \vdots \end{pmatrix} . \tag{2.8}$$

The existence and stability of this minimum will have to be studied on a case by case basis. In this section we assume we are dealing with a model where this type of vacuum is allowed.

We define t_i such that each multiplet has dimension $2t_i + 1$, t_{3Vi} to be the eigenvalue of T_3 when acting on the vacuum of the multiplet, y_i to be the multiplet's hypercharge and $V_i = v_i/\sqrt{2}$.

2.2 The Higgs Mechanism

The Higgs mechanism is the process by which a scalar particle, by developing a vev that breaks a gauge symmetry, gives mass to the gauge boson correspondent to the broken degrees of freedom of that symmetry. To understand this mechanism, let us start by looking at the example of an abelian gauge symmetry, before moving on to the non-abelian case.

2.2.1 Abelian Higgs Mechanism

For the purposes of understanding the Higgs mechanism, let us consider a model with only the abelian gauge group $U(1)$ and a complex scalar particle charged under this symmetry. The covariant derivative takes the form

$$D_\mu \quad = \quad \partial_\mu + ieA_\mu \,, \tag{2.9}$$

and the Higgs potential

$$V(\phi^\pm) = -\mu^2\phi^+\phi^- + \lambda(\phi^+\phi^-)^2 \,. \tag{2.10}$$

This potential has the form of a champagne-bottle profile, with the minimum outside of the centre and spontaneously breaking the $U(1)$ symmetry. The vacuum can the be taken real and assigned the value $v = \sqrt{\mu^2/\lambda}$.

The scalar can be rewritten around the vacuum as

$$\phi^+ = \frac{1}{\sqrt{2}}(v + h + ia) \,, \tag{2.11}$$

and, by expanding the potential, we get

$$V(h,a) = \lambda v^2 h^2 + \lambda v h^3 + \lambda v h a^2 + \frac{\lambda}{4}(h^2 + a^2)^2 - \frac{\lambda v^4}{4} \,. \tag{2.12}$$

Note that there is no term quadratic in the real scalar a, and thus, it is a massless field. The presence of such a massless field is ensured by the Goldstone theorem which states that for each broken degree of freedom of the original symmetry, a massless spinless field shall arise. This field is called a Goldstone boson, and is essential for the Higgs mechanism to take place.

Meanwhile, the covariant derivative acting on the scalar gives

$$D^\mu\phi^+ = \frac{1}{\sqrt{2}}\left(\partial^\mu h + i\partial^\mu a + ieA^\mu(v + h + ia)\right) \,, \tag{2.13}$$

and, keeping only quadratic terms, the kinetic part of the Lagrangian becomes

$$\mathcal{L}_{K2} = |D^\mu\phi^+|^2 = \frac{1}{2}\left(\partial^\mu h\partial_\mu h + \partial^\mu a\partial_\mu a + e^2v^2A^\mu A_\mu + 2evA^\mu\partial_\mu a\right) \,. \tag{2.14}$$

Before the spontaneous breaking of the gauge symmetry, the gauge boson A^μ was massless since one cannot add a mass term while preserving the gauge symmetry. And, by solving the massless Proca equation, one knows that such a field has only two degrees of freedom, corresponding to what we call the two transverse polarisations of the photon in electromagnetism.

Once the symmetry is spontaneously broken, one finds in Equation (2.14) a mass term with $m = ev$. But, by solving the complete Proca equation, one knows that a massive spin-1 field has three degrees of freedom, the two transverse plus a longitudinal one. Since the number of physical degrees of freedom

cannot change between high energies, where the symmetry is not broken, and low energies, where the symmetry is broken, this additional degree of freedom must come from somewhere.

To solve this problem, one can start by noticing that Equation (2.14) can be rearranged as

$$\mathcal{L}_{K2} = \frac{1}{2}\left(\partial^\mu h \partial_\mu h + e^2 v^2 \left(A^\mu + \frac{1}{e}\partial^\mu a\right)\left(A_\mu + \frac{1}{e}\partial_\mu a\right)\right) . \tag{2.15}$$

Using the fact that a $U(1)$ gauge field is free to be redefined with the transformation $A_\mu \to A_\mu + i\partial_\mu\theta$, one can now define the field

$$B^\mu = A^\mu + \frac{1}{e}\partial^\mu a\,, \tag{2.16}$$

leaving $\mathcal{L}_K$ as

$$\mathcal{L}_{K2} = \frac{1}{2}\left(\partial^\mu h \partial_\mu h + e^2 v^2 B^\mu B_\mu\right) . \tag{2.17}$$

As can be seen, the kinetic term of the goldstone boson a, responsible for the dynamics of the field, completely disappeared from the Lagrangian, and we are left with a spin-1 massive boson B^μ in the place of the original A^μ. It is then said that the dynamical degree of freedom of the goldstone boson got absorbed by the originally massless gauge boson to become the longitudinal component of the now massive gauge boson. This process is what is called the Higgs mechanism, and it is the only known way to generate mass to spin-1 fields in renormalizable theories.

2.2.2 Non-Abelian Higgs Mechanism

Let us now consider a theory as the ones described in Section 2.1, but only with one multiplet in Equation (2.8), and losing its subscript. To find the masses of the Gauge bosons, one needs not to look at the Higgs potential, since the Goldstone theorem guarantees that the required Goldstone bosons to be absorbed by the Gauge bosons will appear in the needed fashion. We then jump to the kinetic Lagrangian, and will calculate merely the terms with only neutral particles.

$$\mathcal{L}_{K0} = \frac{1}{2}(\partial^\mu - igt_{3V}W^{3\mu} - ig'yB^\mu)(v + h - ia)(\partial_\mu + igt_{3V}W^3_\mu + ig'yB_\mu)(v + h + ia)\,. \tag{2.18}$$

Taking the scalar fields to zero, one finds the Gauge boson mass terms

$$\mathcal{L}_{M0} = \frac{v^2}{2}(gt_{3V}W^{3\mu} + g'yB^\mu)(gt_{3V}W^3_\mu + g'yB_\mu)\,, \tag{2.19}$$

which corresponds to a mass matrix, in the basis (W^3_μ, B_μ), of

$$M^2 = v^2\begin{pmatrix} g^2t^2_{3V} & gg't_{3V}y \\ gg't_{3V}y & g'^2y^2 \end{pmatrix}\,, \tag{2.20}$$

which in turn needs to be diagonalized. But, looking at Equation (2.19), one infers that the combination

$$Z_\mu = -\frac{1}{\sqrt{g^2 t_{3V}^2 + g'^2 y^2}} \left(g\, t_{3V} W_\mu^3 + g' y B_\mu \right) , \tag{2.21}$$

is an eigenvector with eigenvalue

$$m_Z^2 = v^2 (g^2 t_{3V}^2 + g'^2 y^2) , \tag{2.22}$$

and, since the matrix is hermitian, the perpendicular vector is the other eigenvector with null eigenvalue. One can then define the rotation angle θ_W as

$$\cos(\theta_W) = -\frac{g\, t_{3V}}{\sqrt{g^2 t_{3V}^2 + g'^2 y^2}} , \tag{2.23}$$

$$\sin(\theta_W) = \frac{g' y}{\sqrt{g^2 t_{3V}^2 + g'^2 y^2}} , \tag{2.24}$$

so that:

$$Z_\mu = \cos(\theta_W) W_\mu^3 - \sin(\theta_W) B_\mu , \tag{2.25}$$

$$A_\mu = \sin(\theta_W) W_\mu^3 + \cos(\theta_W) B_\mu , \tag{2.26}$$

where the sign notation was chosen so that the above equations coincide with the definition of the Weinberg angle in the case of the SM.

Calculating the mass term for the charged bosons one finds

$$\mathcal{L}_{M1} = \frac{g^2 v^2}{2} (t(t+1) - t_{3V}^2) W^{+\mu} W_\mu^- , \tag{2.27}$$

leading to a mass of

$$m_W^2 = \frac{g^2 v^2}{2} (t(t+1) - t_{3V}^2) . \tag{2.28}$$

And a procedure like the one in the previous subsection reveals the absorbed goldstone bosons to be a for the Z_μ and a combination of the $H^\pm$ and $\tilde{H}^\pm$ for the $W_\mu^\pm$.

Notice that there is no mass term for A_μ, and so, the resulting terms are still invariant under an abelian gauge transformation on A_μ, which means that there remains an unbroken $U(1)$ gauge symmetry in our theory. To find the corresponding unbroken charge, one needs to apply the field rotation to K_μ, which leads to

$$K_\mu = g(T_+ W_\mu^+ + T_- W_\mu^-) - \frac{g^2 t_{3V} T_3 + g'^2 y Y}{\sqrt{g^2 t_{3V}^2 + g'^2 y^2}} Z_\mu + \frac{g g' (y T_3 - t_{3V} Y)}{\sqrt{g^2 t_{3V}^2 + g'^2 y^2}} A_\mu , \tag{2.29}$$

and, using the useful convention

$$e = \frac{g g'}{\sqrt{g^2 (t_{3V}/y)^2 + g'^2}} \,, \tag{2.30}$$

it can be written as

$$K_\mu = g(T_+ W_\mu^+ + T_- W_\mu^-) - \frac{g^2 t_{3V} T_3 + g'^2 y Y}{\sqrt{g^2 t_{3V}^2 + g'^2 y^2}} Z_\mu + e \left(T_3 - \frac{t_{3V}}{y} Y \right) A_\mu \,. \tag{2.31}$$

The unbroken $U(1)$ charge is then

$$Q = T_3 - \frac{t_{3V}}{y} Y \,. \tag{2.32}$$

This remaining symmetry is usually denoted by $U_{em}(1)$, since its gauge boson A_μ, called the photon, is responsible for electromagnetic interactions. And Q is then the electric charge operator.

To finalise this subsection we note that in the case of the SM one has a doublet with quantum numbers $y = -t_{3V} = 1/2$ which lead to

$$Q = T_3 + Y \,, \tag{2.33}$$

as the reader might be familiar from traditional textbooks.

2.3 Charge Definition in Multi-Higgs

Electric charge is, in a general sense, a combination of the diagonal operators in the covariant derivative. This is the case since there is no flavour changing processes assigned to the electromagnetic force. In the case of $SU(2)_L \times U(1)_Y$, it can then be written as

$$Q = T_3 + rY \,, \tag{2.34}$$

where we used the fact that an overall constant can always be absorbed by e to assign a unitary value to the coefficient of T_3. By definition, this must correspond to the unbroken part of the symmetry, which means that, in models with various scalar multiplets, when applied to the vacuum of these, the charge must vanish

$$Q < \phi_i >= (t_{3Vi} + r y_i) < \phi_i >= 0 \,. \tag{2.35}$$

Since by defining the size of a multiplet and which entry develops the vacuum one already fixes t_{3Vi}, the previous relation holds only if the hypercharges of the multiplets with vacuum satisfy

$$r y_i = -t_{3Vi} \,. \tag{2.36}$$

This means that, when assigning hypercharges to the doublets of a theory, one really only has one degree of freedom to choose, r, and all the hypercharges are automatically assigned in order not to break the electromagnetic gauge symmetry. Note that if another entry of a multiplet were to develop a vacuum, they would not be able to both satisfy Equation (2.36) at the same time, since they would have same y_i but different t_{3Vi}.

With various multiplets, the gauge boson mass terms of the Lagrangian become just a sum of the term from each vacuum

$$\mathcal{L}_M = \sum_i \frac{g^2 v_i^2}{2}(t_i(t_i+1) - t_{3Vi}^2)W^{+\mu}W_\mu^- + \sum_i \frac{v_i^2}{2}(g t_{3Vi} W_\mu^3 + g' y_i B_\mu)^2 \,, \tag{2.37}$$

leading to a charged bosons mass of

$$m_W^2 = \sum_i \frac{g^2 v_i^2}{2}(t_i(t_i+1) - t_{3Vi}^2) \,, \tag{2.38}$$

and a neutral gauge bosons mass matrix of

$$M^2 = \begin{pmatrix} \sum_i g^2 t_{3Vi}^2 v_i^2 & \sum_i g\, t_{3Vi} g' y_i v_i^2 \\ \sum_i g\, t_{3Vi} g' y_i v_i^2 & \sum_i g'^2 y_i^2 v_i^2 \end{pmatrix} \,. \tag{2.39}$$

This matrix has, in general, non-null eigenvalues. But it is easy to check that the condition of Equation (2.36) is enough to render its determinant null, creating one vanishing eigenvalue as expected. In fact, applying those conditions on the Lagrangian leads to

$$\mathcal{L}_M = \sum_i \frac{g^2 v_i^2}{2}(t_i(t_i+1) - t_{3Vi}^2)W^{+\mu}W_\mu^- + \frac{1}{2}(-rgW_\mu^3 + g'B_\mu)^2 \sum_i y_i^2 v_i^2 \,, \tag{2.40}$$

which induces us to generalise the rotation angle to

$$\cos(\theta_W) = \frac{rg}{\sqrt{r^2 g^2 + g'^2}} \,, \tag{2.41}$$

$$\sin(\theta_W) = \frac{g'}{\sqrt{r^2 g^2 + g'^2}} \,, \tag{2.42}$$

leading to

$$\mathcal{L}_M = \sum_i \frac{g^2 v_i^2}{2}(t_i(t_i+1) - t_{3Vi}^2)W^{+\mu}W_\mu^- + \frac{r^2 g^2 + g'^2}{2} Z^\mu Z_\mu \sum_i y_i^2 v_i^2 \,, \tag{2.43}$$

and translating to a mass for the neutral gauge boson of

$$m_Z^2 = (r^2 g^2 + g'^2) \sum_i y_i^2 V_i^2 \,. \tag{2.44}$$

For completion, in order for Equation (2.34) to be valid, we need to explicitly state the generalised

definition

$$e = \frac{gg'}{\sqrt{g^2 r^2 + g'^2}} \,. \tag{2.45}$$

2.4 Custodial Symmetry

In order to understand custodial symmetry, we will start by exemplifying the matter with the case of the doublet.

The doublet can be parameterised as

$$\phi = \frac{1}{\sqrt{2}} \begin{pmatrix} \varphi_1 + i\varphi_2 \\ \varphi_3 + i\varphi_4 \end{pmatrix} \,, \tag{2.46}$$

where the φ_i are real fields, and the most general Higgs potential may be written as

$$V(\phi) = -\mu^2 \phi^\dagger \phi + \lambda (\phi^\dagger \phi)^2 \,. \tag{2.47}$$

The potential only depends on the quantity

$$\phi^\dagger \phi = \frac{1}{2} \left(\varphi_1^2 + \varphi_2^2 + \varphi_3^2 + \varphi_4^2 \right) \,, \tag{2.48}$$

and so, it is not only globally invariant under the $SU(2)_L$ symmetry, but it is actually globally invariant under the larger symmetry group $SO(4)$ that rotates the four scalars between each other. This group is isomorphic to $SU(2)_L \times SU(2)_R$, and, assuming the right hand fermions transform as doublets under $SU(2)_R$, the rest of the SM Lagrangian is also invariant under the larger group.

Since only one of these scalars develops a vacuum, the symmetry breaks to the $SO(3)$ that rotates the remaining three fields and is isomorphic to $SU(2)_V$, the diagonal component of $SU(2)_L \times SU(2)_R$. This remaining global symmetry is the custodial symmetry.

Those three scalars that do not develop a vacuum are the goldstone bosons that will be absorved throughout the Higgs mechanism by the gauge bosons. And, since they transform as a triplet under the custodial symmetry, so must the massive gauge bosons. The presence of custodial symmetry can then be checked for in the mass terms appearing after symmetry breaking and ignoring the mixing with the $U(1)_Y$ gauge boson.

From Equation (2.37) one can obtain

$$\mathcal{L}_M = \sum_i \frac{g^2 v_i^2}{4} (t_i(t_i+1) - t_{3Vi}^2)(W^{1\mu} W_\mu^1 + W^{2\mu} W_\mu^2) + \sum_i \frac{g^2 v_i^2}{2} t_{3Vi}^2 W^{3\mu} W_\mu^3 \,, \tag{2.49}$$

and so, for the theory to be invariant under the global custodial symmetry, since the gauge bosons must transform as a triplet under $SO(3)$, one must have

$$t_i(t_i+1) - t_{3Vi}^2 = 2t_{3Vi}^2 \,, \tag{2.50}$$

for all multiplets in the theory.

The reasoning behind ignoring the $U(1)_Y$ gauge boson in this analysis, is because the $U(1)_Y$ symmetry is actually a subgroup of the global $SO(4)$ symmetry of the potential. Since it is independent of $SU(2)_L$, it must be present as a subgroup in the remaining custodial symmetry group, after symmetry breaking. By gauging only that part of the remaining symmetry, one is breaking the symmetry even further. Nonetheless, the custodial symmetry remains intact in the Higgs sector, since the gauge boson has no influence in it. One must then study the theory without the $U(1)_Y$ gauge boson to obtain the right conditions, since by adding it, one does not change the global symmetries of the Higgs potential.

One can now translate this condition to experimentally measurable consequences, by defining the quantity

$$\rho = \frac{m_W^2}{m_Z^2 \cos^2 \theta_W} \,. \tag{2.51}$$

Using Equations (2.38), (2.41) and (2.44), and after a little algebra, one finds that

$$\rho = \frac{t(t+1) - t_{3V}^2}{2t_{3V}^2} \,, \tag{2.52}$$

for theories with only one scalar, and

$$\rho = \frac{\sum_i (t_i(t_i+1) - t_{3Vi}^2) v_i}{\sum_i 2t_{3Vi}^2 v_i} \,, \tag{2.53}$$

for theories with multiple scalars.

The condition for custodial symmetry is then for the quantity ρ to be measured equal to 1. In fact, this quantity has been measured to extreme precision to a value astonishingly close to that: 1.00038 ± 0.00020[37]. The multiplets included in our theories must then satisfy Equation (2.50) or have a very small vacuum.

The multiplets that satisfy those conditions are the ones with quantum numbers

$$(2t+1, t_{3V}) \in \{(1,0), (2, \pm 1/2), (7 \pm 2), (26, \pm 15/2), (97, \pm 28), ...\} \,, \tag{2.54}$$

and, in this work, we will restrict ourselves to theories including only the first two.

Chapter 3

Multi-Higgs Models

In this chapter we look into more specific multi-Higgs models studied in this work. We start by reviewing the SM. Then, we move on to study models with an arbitrary number of doublets and singlets. We identify an overlooked coupling appearing in some doublet singlet models and motivate the study of experimental signatures of such type of couplings. We end the chapter by studying the Zee model since Zee-type models are the minimal models with the presence of such couplings which will be used in the next chapter to study its possible experimental signatures.

All these models have the structure described in Section 2.1. And so, there is a need only to specify the Higgs content.

3.1 The Standard Model

The SM has only an $SU(2)_L$ doublet. Its vacuum can be brought by an $SU(2)_L$ transformation to the real part of its lower component, leading us to $y = -t_{3V} = 1/2$ as discussed in the last chapter. It can be parameterized as

$$\phi = \begin{pmatrix} G^+ \\ \frac{1}{\sqrt{2}}\left(v + h + iG^0\right) \end{pmatrix} . \tag{3.1}$$

The Higgs potential is the one used in Section 2.4

$$V(\phi) = -\mu^2 \phi^\dagger \phi + \lambda (\phi^\dagger \phi)^2 , \tag{3.2}$$

and, by conducting its derivatives with relation to the scalars, one finds that the vacuum must satisfy

$$v = \sqrt{\frac{\mu^2}{\lambda}} . \tag{3.3}$$

The fields $G^\pm$ and G^0 become the goldstone bosons absorbed by $W^\pm$ and Z respectively. Using the minimum condition in Equation (3.3), the mass of the remaining scalar h, known as the Higgs boson, is

found to be

$$m_h^2 = 2\lambda v^2 \,. \tag{3.4}$$

Since there is only one doublet, the Yukawa sector can only be

$$-\mathcal{L}_Y = \bar{Q}_L \; \tilde{\phi} Y_u u_R + \bar{Q}_L \; \phi Y_d d_R + \bar{L}_L \; \phi Y_e e_R + h.c. \,. \tag{3.5}$$

where

$$\tilde{\phi} = \phi^T i\sigma_2 \tag{3.6}$$

3.2 General Doublet Singlet Models

We consider the models studied in [19] and use a similar notation to the one presented there. The scalar part of the model consists of n_d doublets of $SU(2)$, n_c singly charged singlets and n_n real neutral singlets. The fermionic and vector fields are identical to the SM content.

The scalars are denoted by

$$\begin{aligned} \phi_a &= \begin{pmatrix} \varphi_a^+ \\ \varphi_a^0 \end{pmatrix}, \quad a = 1, 2, ..., n_d \,, \\ \chi_i^+, &\quad i = 1, 2, ..., n_c \,, \\ \chi_r^0, &\quad r = 1, 2, ..., n_n \,, \end{aligned} \tag{3.7}$$

and the neutral fields can be expanded around their vevs as

$$\begin{aligned} \varphi_a^0 &= \frac{1}{\sqrt{2}}(v_a + \varphi_a^{0\prime}) \,, \\ \chi_r^0 &= u_r + \chi_r^{0\prime} \,, \end{aligned} \tag{3.8}$$

with complex v_a and real u_r, where the former satisfy $v = \left(\sum |v_a|^2\right) \simeq 246\text{GeV}$. With a total of $n = n_d + n_c$ complex singly charged scalar fields and $m = 2n_d + n_n$ real neutral scalar fields, we can define the change to the physical basis S_α^+ $(\alpha = 1, 2, ..., n)$ and S_β^0 $(\beta = 1, 2, ..., m)$ with masses $m_{\pm\alpha}$ and $m_{0\beta}$ respectively, throughout the transformations

$$\begin{aligned} \varphi_a^+ &= U_a^\alpha S_\alpha^+ \,, \\ \chi_i^+ &= T_i^\alpha S_\alpha^+ \,, \\ \varphi_a^{0\prime} &= V_a^\beta S_\beta^0 \,, \\ \chi_r^{0\prime} &= R_r^\beta S_\beta^0 \,, \end{aligned} \tag{3.9}$$

where the last matrix is real and the others are complex. In this text, every index appearing up and down

in the same expression is assumed to be summed over. The matrices

$$\tilde{U}^{\alpha}_{\alpha'} = \begin{pmatrix} U^{\alpha}_{a} \\ T^{\alpha}_{i} \end{pmatrix} ,$$

$$\tilde{V}^{\beta}_{\beta'} = \begin{pmatrix} \text{Re } V^{\beta}_{a} \\ \text{Im } V^{\beta}_{a} \\ R^{\beta}_{r} \end{pmatrix} , \tag{3.10}$$

are, respectively, the unitary and orthogonal matrices that diagonalize the charged and neutral mass matrices. The physical fields with indices $\alpha = 1$ and $\beta = 1$ are assigned to the unphysical Goldstone bosons, and the neutral S^0_2 field is assigned to the Higgs particle measured at the LHC with mass $m_h \simeq 125$GeV. We note that even though the matrices defined in Equation (3.10) are unitary, the matrices in Equation (3.9) do not need to be. In fact, only if there is no mixing between the doublet fields and the charged singlets, can the matrices be brought to a basis where they become composed of zeros surrounding a unitary square matrix. This characteristic is of significant importance as we will show later.

3.2.1 Scalar potential

For simplicity, we assume a discrete symmetry under which all fields transform trivially, except the neutral singlet scalars, for which $\chi^0_r \to -\chi^0_r$. The scalar potential may then be conveniently written as

$$\begin{aligned} V = {} & \mu_1^{ab}\phi_a^\dagger\phi_b + \mu_2^{ij}\chi_i^+\chi_j^- + \mu_3^{rs}\chi_r^0\chi_s^0 + (\mu_4^{abi}\phi_a i\sigma_2\phi_b\chi_i^- + h.c.) \\ & + \lambda_1^{abcd}\phi_a^\dagger\phi_b\phi_c^\dagger\phi_d + \lambda_2^{ijkl}\chi_i^+\chi_j^-\chi_k^+\chi_l^- + \lambda_3^{rstu}\chi_r^0\chi_s^0\chi_t^0\chi_u^0 \\ & + \lambda_4^{abij}\phi_a^\dagger\phi_b\chi_i^+\chi_j^- + \lambda_5^{abrs}\phi_a^\dagger\phi_b\chi_r^0\chi_s^0 + \lambda_6^{ijrs}\chi_i^+\chi_j^-\chi_r^0\chi_s^0 , \end{aligned} \tag{3.11}$$

where σ_2 is the second Pauli matrix, μ_3 and λ_3 are real and the rest complex, while $h.c.$ stands for hermitian conjugate. The parameters are subject to the relations

$$\mu_1^{ab} = \mu_1^{ba*} , \qquad \mu_2^{ij} = \mu_2^{ji*} , \qquad \mu_3^{rs} = \mu_3^{sr} , \qquad \mu_4^{abi} = -\mu_4^{bai} ,$$

and

$$\begin{aligned} & \lambda_1^{abcd} = \lambda_1^{cdab} = \lambda_1^{badc*}, \quad \lambda_2^{ijkl} = \lambda_2^{klij} = \lambda_2^{jilk*}, \quad \lambda_3^{rstu} = \lambda_3^{(rstu)}, \\ & \lambda_4^{abij} = \lambda_4^{baji*}, \qquad \lambda_5^{abrs} = \lambda_5^{bars*} = \lambda_5^{absr}, \quad \lambda_6^{ijrs} = \lambda_6^{jirs*} = \lambda_6^{ijsr} , \end{aligned} \tag{3.12}$$

where $(rstu)$ stands for any permutation of the indices $rstu$. After expanding around the vevs with Equation (3.8) and using Equations (3.9)-(3.10) we are interested in the cubic terms

$$
\begin{aligned}
V \supset & \lambda_1^{abcd}(\varphi_a^{0\prime *} v_b + v_a^* \varphi_b^{0\prime})\varphi_c^- \varphi_d^+ + \frac{1}{2}\lambda_4^{abij}(\varphi_a^{0\prime *} v_b + v_a^* \varphi_b^{0\prime})\chi_i^+ \chi_j^- \\
& + 2u_s \lambda_5^{abrs} \varphi_a^- \varphi_b^+ \chi_r^{0\prime} + 2u_s \lambda_6^{ijrs} \chi_i^+ \chi_j^- \chi_r^{0\prime} \qquad (3.13) \\
& \frac{\mu_4^{abi}}{\sqrt{2}}(\varphi_a^+ \varphi_b^{0\prime} - \varphi_a^{0\prime} \varphi_b^+)\chi_i^- + \frac{\mu_4^{abi*}}{\sqrt{2}}(\varphi_a^- \varphi_b^{0\prime *} - \varphi_a^{0\prime *} \varphi_b^-)\chi_i^+ \\
= & \Big[\lambda_1^{abcd}(V_a^{\beta *} v_b + v_a^* V_b^\beta) U_c^{\alpha_1 *} U_d^{\alpha_2} + \frac{1}{2}\lambda_4^{abij}(V_a^{\beta *} v_b + v_a^* V_b^\beta) T_i^{\alpha_1} T_j^{\alpha_2 *} \\
& + 2u_s \lambda_5^{abrs} U_a^{\alpha_1 *} U_b^{\alpha_2} R_r^\beta + 2u_s \lambda_6^{ijrs} T_i^{\alpha_1} T_j^{\alpha_2 *} R_r^\beta \qquad (3.14) \\
& \frac{\mu_4^{abi}}{\sqrt{2}}(U_a^{\alpha_1} V_b^\beta - V_a^\beta U_b^{\alpha_1}) T_i^{\alpha_2 *} + \frac{\mu_4^{abi*}}{\sqrt{2}}(U_a^{\alpha_2 *} V_b^{\beta *} - V_a^{\beta *} U_b^{\alpha_2 *}) T_i^{\alpha_1} \Big] S_{\alpha_1}^+ S_{\alpha_2}^- S_\beta^0 \\
\equiv & g^{\beta \alpha_1 \alpha_2}\, v\, S_{\alpha_1}^+ S_{\alpha_2}^- S_\beta^0 \,,
\end{aligned}
$$

and in the quadratic terms with charged scalars, given by

$$
\begin{aligned}
V \supset & (\mu_1^{ab} + \lambda_1^{abcd} v_d v_c^* + \lambda_5^{abrs} u_r u_s)\varphi_b^+ \varphi_a^- + (\mu_2^{ij} + \frac{1}{2}\lambda_4^{abij} v_b v_a^* + \lambda_6^{ijrs} u_r u_s)\chi_i^+ \chi_j^- \\
& + \frac{\mu_4^{abi}}{\sqrt{2}}(v_a \varphi_b^+ - v_b \varphi_a^+)\chi_i^- + \frac{\mu_4^{abi*}}{\sqrt{2}}(v_a^* \varphi_b^- - v_b^* \varphi_a^-)\chi_i^+ \qquad (3.15) \\
= & \Big[\left(\mu_1^{ab} + \lambda_1^{abcd} v_d v_c^* + \lambda_5^{abrs} u_r u_s\right) U_b^{\alpha_1} U_a^{\alpha_2 *} + \left(\mu_2^{ij} + \frac{1}{2}\lambda_4^{abij} v_b v_a^* + \lambda_6^{ijrs} u_r u_s\right) T_i^{\alpha_1} T_j^{\alpha_2 *} \\
& + \frac{\mu_4^{abi}}{\sqrt{2}}\left(v_a U_b^{\alpha_1} - v_b U_a^{\alpha_1}\right) T_i^{\alpha_2 *} + \frac{\mu_4^{abi*}}{\sqrt{2}}\left(v_a^* U_b^{\alpha_2 *} - v_b^* U_a^{\alpha_2 *}\right) T_i^{\alpha_1} \Big] S_{\alpha_1}^+ S_{\alpha_2}^- \,. \qquad (3.16)
\end{aligned}
$$

We see from Equation (3.15) that there is no mixing between the charged fields originating from doublets with the charged fields originating from singlets, unless $\mu_4^{abi} \neq 0$ for some combination of indices. Thus, the cubic terms in the potential (3.11) are essential for the non-unitary behaviour of the matrix U_a^α that will be shown to be mandatory for the appearance of $Z H_1^+ H_2^-$ couplings that change the "flavour" of the charged scalars. Also, Equation (3.13) tells us that the coupling $h^0 H_1^+ H_2^-$ exists with $\mu_4^{abi} = 0$ only for H_1^+ and H_2^+ belonging both to the doublet sector or both to the singlet sector, while only $\mu_4^{abi} \neq 0$ induces a mixing of the sectors. Since μ_4^{abi} is anti-symmetric in (a, b), the minimal scalar sector containing such a coupling is a model with two doublets and one charged singlet. This corresponds to the Zee-type models, which we study in the next section.

3.2.2 Gauge-scalar couplings

The part of the Lagrangian regarding the covariant derivative of the scalars, was derived in Equation (29) of [19]. The relevant terms for our purposes are

$$\begin{aligned}\mathcal{L} \supset\ & ieA_\mu\delta^{\alpha\alpha'}(S^+_\alpha\partial^\mu S^-_{\alpha'} - S^-_{\alpha'}\partial^\mu S^+_\alpha) + e^2A_\mu A^\mu\delta^{\alpha\alpha'}S^-_{\alpha'}S^+_\alpha \\ & + g\left(M_W W^+_\mu W^{-\mu} + \frac{M_Z}{2c_W}Z_\mu Z^\mu\right)\mathrm{Re}(\omega^\dagger V)^\beta S^0_\beta - i\frac{g}{2c_W}Z_\mu(2s^2_W\delta^{\alpha\alpha'} \\ & - (U^\dagger U)^{\alpha'\alpha})(S^+_\alpha\partial^\mu S^-_{\alpha'} - S^-_{\alpha'}\partial^\mu S^+_\alpha) - \frac{eg}{c_W}A_\mu Z^\mu(2s^2_W\delta^{\alpha\alpha'} - (U^\dagger U)^{\alpha'\alpha})S^-_{\alpha'}S^+_\alpha\,, \end{aligned} \tag{3.17}$$

where $\omega_a = v_a/v$. Here we finally check the appearance of the expression $(U^\dagger U)^{\alpha'\alpha}$ that is diagonal if U^α_a is unitary. In models without a μ_4^{abi} coupling, this expression will then be diagonal and there will be no "flavour" changing $ZH_1^+H_2^-$ coupling. The exploration of this under-appreciated point is one of the distinguishing features of this work.

3.2.3 Fermion-scalar couplings

The Yukawa Lagrangian is the same as for the NHDM for $N = n_d$, and the fermion-scalar couplings were calculated for that model in [20]. The calculation for our model proceeds in a similar fashion, leaving us with the relevant Lagrangian term

$$\begin{aligned}\mathcal{L} \supset\ & -\frac{1}{v}\bar{d}_L\left(N^\alpha_d B^\beta_\alpha S^0_\beta\right)d_R - \frac{1}{v}\bar{u}_L\left(N^\alpha_u B^{\beta*}_\alpha S^0_\beta\right)u_R - \frac{1}{v}\bar{e}_L\left(N^\alpha_e B^\beta_\alpha S^0_\beta\right)e_R \\ & - \bar{u}_L V\left(N^\alpha_d S^+_\alpha\right)d_R + \bar{d}_L V^\dagger\left(N^\alpha_u S^-_\alpha\right)u_R + \text{h.c.}\,, \end{aligned} \tag{3.18}$$

where

$$\begin{aligned} B^\beta_\alpha &= U^{\dagger a}_\alpha V^\beta_a, & N^\alpha_d &= \frac{v}{\sqrt{2}}U^\dagger_{dL}\Gamma^a U_{dR}U^\alpha_a\,, \\ N^\alpha_u &= \frac{v}{\sqrt{2}}U^\dagger_{uL}\Delta^a U_{uR}U^{\alpha*}_a, & N^\alpha_e &= \frac{v}{\sqrt{2}}U^\dagger_{eL}\Gamma^a_e U_{eR}U^\alpha_a\,, \end{aligned} \tag{3.19}$$

V is the CKM matrix, Γ^a, Δ^a and Γ^a_e are the Yukawa coupling matrices, and $U_{fL/R}$ are the rotation matrices to the physical basis. We ignore neutrino masses for simplicity. To calculate the Higgs decays, the relevant terms may be written as

$$\mathcal{L} \supset -\sum_f\left(\sqrt{2}G_\mu\right)^{\frac{1}{2}} m_f\bar{\psi}_f(a^\beta_f + i\gamma_5 b^\beta_f)\psi_f S^0_\beta\,, \tag{3.20}$$

where m_f are the fermion masses, G_μ is the Fermi constant, satisfying $\left(\sqrt{2}G_\mu\right)^{-\frac{1}{2}} = v$, and

$$\begin{aligned} a_f^\beta &= \frac{v}{2m_f}(R^{f\beta} + L^{f\beta})\,, \qquad b_f^\beta = -i\frac{v}{2m_f}(R^{f\beta} + L^{f\beta})\,, \\ R^{f\beta} &= \frac{1}{v}N_f^\alpha B_\alpha^\beta\,, \qquad L^{f\beta} = \frac{1}{v}N_f^{\dagger\alpha} B_\alpha^{\beta *}\,, \qquad f = d, e\,, \\ R^{u\beta} &= \frac{1}{v}N_u^\alpha B_\alpha^{\beta *}\,, \qquad L^{u\beta} = \frac{1}{v}N_u^{\dagger\alpha} B_\alpha^{\beta}\,. \end{aligned} \tag{3.21}$$

3.3 Zee-type Models

As an example, we look at a particular case of Zee-type models [8] consisting of a type II 2HDM with a complex singly charged singlet scalar. In a type II 2HDM, the fields satisfy a Z_2 symmetry where ϕ_2 and u_R transform as $\psi \to -\psi$, while the other fields do not transform under the symmetry. This means that ϕ_2 will only couple to the up type quarks while ϕ_1 will only couple to the rest of the fermions.

When using this model in Chapter 4, the purpose is not to make a global fit to the quark, scalar and also the lepton sectors of any specific Zee model, but rather to highlight those features of such types of model that could be probed at LHC. As a result, we do not explore the bounds coming from the lepton sector, including neutrino oscillations; an analysis which can be found, for example, in Refs. [14, 15]. These references simplify the analysis by effectively using the Z_2 symmetry in the quark sector, which is helpful to fix the production and some branching ratios at LHC. Those simulations also assume some scalar couplings to vanish, effectively bringing the result close to that in the Z_2 scalar sector used here. For simplicity, we take couplings consistent with Z_2 in the quark-scalar sectors, reducing the number of parameters to scan, and simplifying the analysis of some theoretical constraints, such as bounded from below (BFB) and absence of charge breaking (CB) vacua. Our main result, the importance of searching for the decay $H_2^+ \to H_1^+ Z$, is not affected by this simplification.

3.3.1 The Higgs potential and rotation matrices

The Higgs potential can in general be written as a particular case of Equation (3.11),

$$\begin{aligned} V = {} & m_C^2\chi^+\chi^- + \lambda_C(\chi^+\chi^-)^2 + \left[\mu_4\ \phi_1 i\sigma_2\phi_2\chi^- + h.c.\right] + m_1^2\phi_1^\dagger\phi_1 + m_2^2\phi_2^\dagger\phi_2 \\ & - m_{12}^2\left(\phi_1^\dagger\phi_2 + \phi_2^\dagger\phi_1\right) + \left[k_1\phi_1^\dagger\phi_1 + k_2\phi_2^\dagger\phi_2 - k_{12}\left(\phi_1^\dagger\phi_2 + \phi_2^\dagger\phi_1\right)\right]\chi^+\chi^- \\ & + \frac{\lambda_1}{2}\left(\phi_1^\dagger\phi_1\right)^2 + \frac{\lambda_2}{2}\left(\phi_2^\dagger\phi_2\right)^2 + \lambda_3\phi_1^\dagger\phi_1\phi_2^\dagger\phi_2 + \lambda_4\phi_1^\dagger\phi_2\phi_2^\dagger\phi_1 + \frac{\lambda_5}{2}\left[\left(\phi_1^\dagger\phi_2\right)^2 + \left(\phi_2^\dagger\phi_1\right)^2\right], \end{aligned} \tag{3.22}$$

where we generalized the 2HDM potential with a Z_2 symmetry in [21]. For simplicity, we consider all parameters and vevs real, corresponding to CP conservation.

Allowing the doublets to develop vevs, the minimum conditions read

$$\begin{aligned} m_1^2 &= \frac{2m_{12}^2 v_2 - v_1^3\lambda_1 - v_1 v_2^2(\lambda_3 + \lambda_4 + \lambda_5)}{2v_1}\,, \\ m_2^2 &= \frac{2m_{12}^2 v_1 - v_2^3\lambda_1 - v_2 v_1^2(\lambda_3 + \lambda_4 + \lambda_5)}{2v_2}\,. \end{aligned} \tag{3.23}$$

The analytic expressions for the mass matrices have no inherent interest, so we will just state some of their properties, while defining the rotation to the physical basis. First, we note that CP-odd fields do not mix with the CP-even fields. The mass matrix for the CP-odd fields has the eigenvectors (v_1, v_2) and $(v_2, -v_1)$, with the first corresponding to a null eigenvalue, which is the Goldstone boson. We can transform the fields into the physical mass basis through[1]

$$\begin{pmatrix} S_1^0 \equiv G^0 \\ S_4^0 \equiv A \end{pmatrix} = \begin{pmatrix} \cos\beta & \sin\beta \\ -\sin\beta & \cos\beta \end{pmatrix} \begin{pmatrix} \mathrm{Im}\varphi_1^{0\prime} \\ \mathrm{Im}\varphi_2^{0\prime} \end{pmatrix} \equiv \mathcal{O}_\beta \begin{pmatrix} \mathrm{Im}\varphi_1^{0\prime} \\ \mathrm{Im}\varphi_2^{0\prime} \end{pmatrix} , \tag{3.24}$$

where

$$\cos\beta = v_1/v, \quad \sin\beta = v_2/v, \quad v = \sqrt{v_1^2 + v_2^2}\,. \tag{3.25}$$

By applying the same rotation to the doublets' charged scalars

$$\begin{pmatrix} S_1^+ \equiv G^+ \\ H^+ \end{pmatrix} = \begin{pmatrix} \cos\beta & \sin\beta \\ -\sin\beta & \cos\beta \end{pmatrix} \begin{pmatrix} \varphi_1^+ \\ \varphi_2^+ \end{pmatrix} , \tag{3.26}$$

we find the charged Goldstone boson G^+, and the intermediate field H^+, not yet a mass eigenstate. Finally, the remaining charged and neutral scalars do not follow such simple relations. So we need to diagonalize, in the general case, with two new independent angles

$$\begin{pmatrix} S_2^0 \\ S_3^0 \end{pmatrix} = \begin{pmatrix} \cos\alpha & \sin\alpha \\ -\sin\alpha & \cos\alpha \end{pmatrix} \begin{pmatrix} \mathrm{Re}\varphi_1^{0\prime} \\ \mathrm{Re}\varphi_2^{0\prime} \end{pmatrix} \equiv \mathcal{O}_\alpha \begin{pmatrix} \mathrm{Re}\varphi_1^{0\prime} \\ \mathrm{Re}\varphi_2^{0\prime} \end{pmatrix} , \tag{3.27}$$

$$\begin{pmatrix} S_2^+ \\ S_3^+ \end{pmatrix} = \begin{pmatrix} \cos\gamma & \sin\gamma \\ -\sin\gamma & \cos\gamma \end{pmatrix} \begin{pmatrix} H^+ \\ \chi^+ \end{pmatrix} \equiv \mathcal{O}_\gamma \begin{pmatrix} H^+ \\ \chi^+ \end{pmatrix} . \tag{3.28}$$

Note that, if we had applied the rotation by β initially to the doublets themselves, we would get to the so-called Higgs basis [22].

Inverting all the transformations and joining the two charged transformation above, we find that the matrices defined in Equations (3.9)-(3.10) are

$$V = \begin{pmatrix} i\cos\beta & \cos\alpha & -\sin\alpha & -i\sin\beta \\ i\sin\beta & \sin\alpha & \cos\alpha & i\cos\beta \end{pmatrix} , \tag{3.29}$$

$$U = \begin{pmatrix} \cos\beta & -\sin\beta\cos\gamma & \sin\beta\sin\gamma \\ \sin\beta & \cos\beta\cos\gamma & -\cos\beta\sin\gamma \end{pmatrix} , \tag{3.30}$$

$$T = \begin{pmatrix} 0 & \sin\gamma & \cos\gamma \end{pmatrix} . \tag{3.31}$$

[1] For convenience, we place the pseudoscalar as the last of the neutral scalars. So S_4^0 is the CP odd scalar and S_2^0, S_3^0 are the two CP even eigenstates. Notice that this choice affects the order of the columns in the matrix V in Equation (3.29).

Some of the relevant combinations of these matrices that appear in the Lagrangian terms calculated in the previous section are

$$U^\dagger U = \begin{pmatrix} 1 & 0 & 0 \\ 0 & \cos^2\gamma & -\sin\gamma\cos\gamma \\ 0 & -\sin\gamma\cos\gamma & \sin^2\gamma \end{pmatrix} , \tag{3.32}$$

$$B = U^\dagger V = \begin{pmatrix} i & \cos(\beta-\alpha) & \sin(\beta-\alpha) & 0 \\ 0 & -\cos\gamma\sin(\beta-\alpha) & \cos\gamma\cos(\beta-\alpha) & i\cos\gamma \\ 0 & \sin\gamma\sin(\beta-\alpha) & -\sin\gamma\cos(\beta-\alpha) & -i\sin\gamma \end{pmatrix} , \tag{3.33}$$

$$\mathrm{Re}\omega^\dagger V = \begin{pmatrix} 0 & \cos(\beta-\alpha) & \sin(\beta-\alpha) & 0 \end{pmatrix} . \tag{3.34}$$

Note that, if we had started by bringing the doublets to the Higgs basis, and then defined α as the rotation of the neutral CP-even fields from that basis to the physical one, then α would transform as $\alpha \to \alpha + \beta$, and these matrices would become independent of β.

The non diagonal nature of $U^\dagger U$ is what gives rise to the flavour changing coupling of the charged scalars with the Z boson, adding a new type of diagrams to the process $h \to Z\gamma$ when compared to the general NHDM. In that same sense, the non mixture of the first component of that matrix with the rest ensures that the Goldstone bosons do not take part on those flavour changing couplings, so that the diagrams involving the W bosons remain safely of the same nature.

3.3.2 The choice of independent parameters

After using the minimisation Equations (3.23) to get v and β, we are left with more twelve real independent parameters in the Higgs potential of Equation (3.22)

$$m_C^2, \lambda_C, \mu_4, m_{12}^2, k_1, k_2, k_{12}, \lambda_1, \lambda_2, \lambda_3, \lambda_4, \lambda_5 . \tag{3.35}$$

For phenomenological studies it is convenient to trade some of these parameters for the physical masses of the neutral and charged scalars: $m_{H_1^0}, m_{H_2^0}, m_{A^0}, m_{H_1^+}$, and $m_{H_2^+}$. This follows a standard procedure. We just give the example of the mass matrix for the pseudo-scalars. We have

$$\mathcal{L} \supset -\frac{1}{2}\left[\mathrm{Im}\varphi_1^{0\prime}, \mathrm{Im}\varphi_2^{0\prime}\right] M_P^2 \begin{bmatrix} \mathrm{Im}\varphi_1^{0\prime} \\ \mathrm{Im}\varphi_2^{0\prime} \end{bmatrix} + \cdots , \tag{3.36}$$

where

$$M_P^2 = \begin{bmatrix} \frac{v_2}{v_1}\left(m_{12}^2 - \lambda_5 v_1 v_2\right) & -m_{12}^2 + \lambda_5 v_1 v_2 \\ -m_{12}^2 + \lambda_5 v_1 v_2 & \frac{v_1}{v_2}\left(m_{12}^2 - \lambda_5 v_1 v_2\right) \end{bmatrix} . \tag{3.37}$$

Now using

$$\begin{bmatrix} \mathrm{Im}\varphi_1^{0\prime} \\ \mathrm{Im}\varphi_2^{0\prime} \end{bmatrix} = \mathcal{O}_\beta^T \begin{bmatrix} G^0 \\ A^0 \end{bmatrix} , \tag{3.38}$$

we obtain

$$\mathcal{O}_\beta M_P^2 \mathcal{O}_\beta^T = \begin{bmatrix} 0 & 0 \\ 0 & m_{A^0}^2 \end{bmatrix} . \tag{3.39}$$

From here we can get λ_5 as a function of the mass m_{A^0} and other independent parameters,

$$\lambda_5 = \frac{1}{v^2}\left(-m_{A^0}^2 + \frac{m_{12}^2}{\sin\beta\cos\beta}\right) . \tag{3.40}$$

Following this procedure for the other mass matrices we can solve for the other λ's as well as for μ_4, m_C^2. We find

$$\lambda_1 = \frac{1}{v^2\cos^2\beta}\left(m_{H_1^0}^2\cos^2\alpha + m_{H_2^0}^2\sin^2\alpha - m_{12}^2\tan\beta\right), \tag{3.41a}$$

$$\lambda_2 = \frac{1}{v^2\sin^2\beta}\left(m_{H_2^0}^2\cos^2\alpha^2 - m_{12}^2\cot\beta + m_{H_1^0}^2\sin^2\alpha\right), \tag{3.41b}$$

$$\lambda_3 = \frac{1}{v^2}\left(2m_{H_1^+}^2\cos^2\gamma + 2m_{H_2^+}^2\sin^2\gamma - \frac{m_{12}^2 + (m_{H_2^0}^2 - m_{H_1^0}^2)\cos\alpha\sin\alpha}{\sin\beta\cos\beta}\right), \tag{3.41c}$$

$$\lambda_4 = -\frac{1}{v^2}\left(\lambda_5 v^2 + 2m_{H_1^+}^2\cos^2\gamma - \frac{2m_{12}^2}{\sin\beta\cos\beta} + 2m_{H_2^+}^2\sin^2\gamma\right), \tag{3.41d}$$

$$\mu_4 = -\frac{\sqrt{2}}{v}(m_{H_1^+}^2 - m_{H_2^+}^2)\cos\gamma\sin\gamma, \tag{3.41e}$$

$$\begin{aligned} m_C^2 = &-\frac{1}{2}k_1 v^2\cos^2\beta + k_{12}v^2\cos\beta\sin\beta \; - \frac{1}{2}k_2 v^2\sin^2\beta \\ &+ m_{H_1^+}^2\sin^2\gamma + m_{H_2^+}^2\cos^2\gamma . \end{aligned} \tag{3.41f}$$

This choice is, of course, not unique but it is a convenient one. In the end, our set of twelve independent parameters is

$$m_{H_1^0}, m_{H_2^0}, m_{A^0}, m_{H_1^+}, m_{H_2^+}, m_{12}^2, \alpha, \gamma, \lambda_C, k_1, k_2, k_{12} . \tag{3.42}$$

3.3.3 Fermion couplings to scalars

The Yukawa couplings to the quarks can be written as

$$-\mathcal{L}_Y = \bar{Q}_L\;\tilde{\phi}_2 Y_u u_R + \bar{Q}_L\;\phi_1 Y_d d_R + h.c. \tag{3.43}$$

Going to the charged physical basis, we find the couplings

$$-\mathcal{L}_Y \supset \frac{\sqrt{2}V_{ud}}{v}\;\bar{u}\left(m_u\xi_A^u P_L + m_d\xi_A^d P_R\right)\,d\,\left(\cos\gamma S_1^+ - \sin\gamma S_2^+\right) + h.c. , \tag{3.44}$$

where, with these definitions,

$$\xi_A^u = \cot\beta , \quad \xi_A^d = \tan\beta . \tag{3.45}$$

These are exactly the 2HDM couplings of fermions to the only charged scalar existent in that case: H^+_{2HDM} [21]. We re-obtain them with the substitution $(\cos\gamma S_1^+ - \sin\gamma S_2^+) \to H^+_{\text{2HDM}}$. Said otherwise, the vertices udS_1^+ and udS_2^+ are the same as the 2HDM vertex udH^+_{2HDM}, but with the factors $\cos\gamma$ and $-\sin\gamma$, respectively. This is not surprising. Indeed, the combination of scalars appearing above corresponds to the H^+ field. This field is the one we find in the doublets when in the Higgs basis and so the result is the same as treating the model as we would treat the 2HDM, and then replace the charged scalar by this combination.

Chapter 4

The Search for Distinctive Signals of Zee-type Models

In this Chapter we further study the Zee model introduced in the last Chapter in order to find an example of a distinctive signal of the flavour changing couplings of the charged scalars with the Z boson discussed before. In Section 4.1 we discuss the constraints, both theoretical and experimental on the model. Our results are presented in Section 4.2 where we discuss the impact on $h \to Z\gamma$ and in Section 4.3 where we study the novel decay $H_2^+ \to H_1^+ Z$. For this decay we propose benchmark points with noteworthy features in Section 4.4.

4.1 Constraints on the Model

4.1.1 Theoretical Constraints

Bounded from Below

The necessary and sufficient conditions for the potential to be bounded from below (BFB) are know [23, 24] for the neutral part of the potential, that coincides with the 2HDM. They are

$$\lambda_1 \geq 0, \quad \lambda_2 \geq 0, \quad \lambda_3 + \sqrt{\lambda_1 \lambda_2} \geq 0, \quad \lambda_3 + \lambda_4 - |\lambda_5| + \sqrt{\lambda_1 \lambda_2} \geq 0\,. \tag{4.1}$$

For the Zee model they were studied in Reference [25]. They extended the conditions in Equation (4.1) but were not able to find necessary and sufficient conditions, only necessary conditions. To explain these conditions it is better to use their notation and indicate the correspondence with ours. They write the quartic part of the potential as

$$\begin{aligned} V_Q =& b_{00}x_0^2 + b_{11}x_1^2 + b_{22}x_2^2 + b_{33}x_3^2 + b_{44}x_4^2 \\ &+ b_{01}x_0x_1 + b_{02}x_0x_2 + b_{03}x_0x_3 + b_{12}x_1x_2 + b_{13}x_1x_3 + b_{23}x_2x_3\,, \end{aligned} \tag{4.2}$$

where

$$x_0 = |\chi^+|^2,\ x_1 = |\phi_1|^2,\ x_2 = |\phi_2|^2,\ x_3 = \mathrm{Re}(\phi_1^\dagger \phi_2),\ x_4 = \mathrm{Im}(\phi_1^\dagger \phi_2)\,. \tag{4.3}$$

Comparing with the potential in Equation (3.22), we obtain

$$\begin{aligned} &b_{00} = \lambda_C,\ b_{11} = \frac{1}{2}\lambda_1,\ b_{22} = \frac{1}{2}\lambda_2,\ b_{33} = \lambda_4 + \lambda_5,\ b_{44} = \lambda_4 - \lambda_5, \\ &b_{01} = k_1,\ b_{02} = k_2,\ b_{03} = -2k_{12},\ b_{12} = \lambda_3,\ b_{13} = 0,\ b_{23} = 0\,. \end{aligned} \tag{4.4}$$

They found the following necessary conditions for the potential to be BFB,

$$b_{11} \geq 0,\ b_{22} \geq 0,\ b_{12} \geq -2\sqrt{b_{11}b_{22}}, b_{12} + b_{44} \geq -2\sqrt{b_{11}b_{22}},\ b_{12} + b_{33} \geq -2\sqrt{b_{11}b_{22}}, \tag{4.5a}$$

$$b_{01} \geq -2\sqrt{b_{00}b_{11}},\ b_{02} \geq -2\sqrt{b_{00}b_{22}},\ f(\alpha,\theta) \geq 0,\ \forall \alpha, \theta. \tag{4.5b}$$

where

$$\begin{aligned} f(\alpha,\theta) = &\frac{1}{8} b_{03} \sin 2\theta \sin^2 2\alpha + \frac{1}{4}\left(b_{01}\cos^2\theta + b_{02}\sin^2\theta\right)\sin^2 2\alpha \\ &+ \left[b_{11}\cos^4\theta + b_{22}\sin^4\theta + \frac{1}{4}\left(b_{12} + b_{33}\right)\sin^2 2\theta\right]\sin^4\alpha\,. \end{aligned} \tag{4.6}$$

It is easy to verify that the conditions in Equation (4.5a) correspond to the usual conditions for the 2HDM in Equation (4.1). The others are new for Zee-type models. The condition in Equation (4.6) cannot be solved analytically for the b_{ij}. Therefore we took a large random sample of θ and α and excluded points that have $f(\alpha,\theta) < 0$. As explained in Reference [25], even after applying these constraints there are a few points that are still not BFB. We have verified this fact when considering the analysis of the charged breaking minima in the following section, and we have also discarded those points.

Charge Breaking Minima

The analysis of the charge breaking (CB) minima is much more complicated that in the 2HDM [24], because of the cubic term in the potential. Indeed, contrary to the 2HDM, the condition

$$V_{CB} > V_N\,, \tag{4.7}$$

is not guaranteed to be verified even when we are at the normal neutral minimum, V_N. As it is very complicated (if not impossible) to solve a set of nonlinear equations for the stationary points of V_{CB}, we took a different approach, based on Reference [25]. We parameterize the possible charge breaking minima as

$$\phi_1 = \begin{bmatrix} y_1 \\ y_2 \end{bmatrix},\ \phi_2 = \begin{bmatrix} y_3 \\ y_4 \end{bmatrix},\ \chi^+ = y_5\,. \tag{4.8}$$

Then, for the parameters for which we have a normal minimum V_N,

$$\text{Set}_{\text{min}} = m_1^2, m_2^2, m_C^2, \lambda_C, \mu_4, m_{12}^2, k_1, k_2, k_{12}, \lambda_1, \lambda_2, \lambda_3, \lambda_4, \lambda_5 \,, \tag{4.9}$$

we consider the function $V_{\text{other}}(\text{Set}_{\text{min}}, y_i)$. We start by taking a large set of random values for y_i

$$y_i \in [-1000, 1000]\,\text{GeV}\,, \tag{4.10}$$

and then for each of these initial values we apply the method of gradient descent to obtain the lowest possible value for $V_{\text{other}}(y_i)$ and compare it with V_N. If $V_N < V_{\text{other}}$ we keep the point. In doing this we also verified the claim [25] that the BFB conditions are not sufficient, as we found a small amount of points corresponding to potentials unbounded from below.

There is a final point deserving a comment. When doing the procedure described above, in many cases we got to a point where $y_5 = 0$ (of course numerically there is no such thing as zero and we have considered $|y_5| < 10^{-6}$). As y_1 and y_3 are non-zero, the question is if this is really a charged breaking minimum or not. We can make an SU(2) rotation to bring to zero the upper component of the first doublet

$$\begin{bmatrix} \cos\theta & \sin\theta \\ -\sin\theta & \cos\theta \end{bmatrix} \begin{bmatrix} y_1 \\ y_2 \end{bmatrix} = \begin{bmatrix} 0 \\ y_2' \end{bmatrix}, \quad \tan\theta = -\frac{y_1}{y_2}\,. \tag{4.11}$$

Now, if the *same* rotation on the second doublet also gives

$$\begin{bmatrix} \cos\theta & \sin\theta \\ -\sin\theta & \cos\theta \end{bmatrix} \begin{bmatrix} y_3 \\ y_4 \end{bmatrix} = \begin{bmatrix} 0 \\ y_4' \end{bmatrix}, \tag{4.12}$$

and

$$\sqrt{y_2'^2 + y_4'^2} = \frac{v}{\sqrt{2}}\,, \tag{4.13}$$

then this is just a normal minimum. In all occasions we found, this was precisely the same normal minimum V_N in a different guise.[1] We have looked at these situations and kept the points if these conditions were verified.

Perturbative Unitarity

To ensure perturbative unitarity of the quartic couplings we implemented the general algorithm presented in Reference [26]. As we are interested in the high energy limit, one just needs to evaluate the scattering S-matrix for the two body scalar bosons, and these arise exclusively from the quartic part of the potential. Since the electric charge and the hypercharge are conserved in this high energy scattering, we can

[1] This explains why we used V_{other} above, and not V_{CB}.

separate the states according to these quantum numbers. In the notation of Reference [26],

$$\phi_i = \begin{bmatrix} w_i^+ \\ n_i \end{bmatrix}, \quad \phi_i^\dagger = \begin{bmatrix} w_i^- \\ n_i^* \end{bmatrix}^T, \quad \chi = \chi^+, \quad \chi^* = \chi^- . \tag{4.14}$$

This corresponds to the following possibilities,

$$Q = 2, Y = 1 \qquad S_\alpha^{++} = \{w_1^+ w_1^+, w_1^+ w_2^+, w_1^+ \chi^+, w_2^+ w_2^+, w_2^+ \chi^+, \chi^+ \chi^+\}, \tag{4.15a}$$

$$Q = 1, Y = 1 \qquad S_\alpha^{+} = \{w_1^+ n_1, w_1^+ n_2, w_2^+ n_1, w_2^+ n_2, \chi^+ n_1, \chi^+ n_2\}, \tag{4.15b}$$

$$Q = 1, Y = 0 \qquad T_\alpha^{+} = \{w_1^+ n_1^*, w_1^+ n_2^*, w_2^+ n_1^*, w_2^+ n_2^*, \chi^+ n_1^*, \chi^+ n_2^*\}, \tag{4.15c}$$

$$Q = 0, Y = 1 \qquad S_\alpha^{0} = \{n_1 n_1, n_1 n_2, n_2 n_2\}, \tag{4.15d}$$

$$Q = 0, Y = 0 \qquad T_\alpha^{0} = \{w_1^- w_1^+, w_1^- w_2^+, w_1^- \chi^+, w_2^- w_1^+, w_2^- w_2^+, w_2^- \chi^+, \chi^- w_1^+, \chi^- \chi^+, \chi^- \chi^+, n_1 n_1^*, n_1 n_2^*, n_2 n_1^*, n_2 n_2^*\}. \tag{4.15e}$$

With this setup we have to find the scattering matrices for each (Q, Y) combination and their eigenvalues. Let us call this set Λ_i. Then the perturbative unitarity constraints are

$$\max(\Lambda_i) < 8\pi, \quad i = 1, \ldots, 19. \tag{4.16}$$

In Appendix C we write explicitly the various scattering matrices and their eigenvalues. In total we have 19 different eigenvalues, as we already anticipated in Equation (4.16).

The oblique parameters S, T, U

All the points in parameter space have to satisfy the electroweak precision measurements, using the oblique parameters S, T and U. We demand that S, T and U are within 2σ of the fit given in [27]. For general models with an arbitrary number of doublets and singlets the expressions for the oblique parameters were given in Refs. [19, 28]. They depend on combinations of the matrices V and U defined in Equations (3.29)-(3.30). The needed matrices are $U^\dagger U$ in Equation (3.32) , $U^\dagger V$ in Equation (3.33), and

$$\mathrm{Im} V^\dagger V = \begin{pmatrix} 0 & -\cos(\beta-\alpha) & -\sin(\beta-\alpha) & 0 \\ \cos(\beta-\alpha) & 0 & 0 & -\sin(\beta-\alpha) \\ \sin(\beta-\alpha) & 0 & 0 & \cos(\beta-\alpha) \\ 0 & \sin(\beta-\alpha) & -\cos(\beta-\alpha) & 0 \end{pmatrix}. \tag{4.17}$$

4.1.2 Constraints from the LHC

From the LHC data we have two types of constraints. First we consider the constraints on the h_{125} Higgs boson. These are normally enforced through the signals strengths for each production mode $i = \mathtt{ggF}, \mathtt{VBF}, \mathtt{VH}, \mathtt{ttH}$ and final state $j = H \to \gamma\gamma, H \to ZZ, H \to ZZ, H \to \tau\tau, H \to bb$, and are defined

by

$$\mu_{ij} = \frac{\sigma_i(pp \to H)}{\sigma_i^{\rm SM}(pp \to H)} \frac{\mathrm{BR}(H \to j)}{\mathrm{BR}^{\rm SM}(H \to j)} \tag{4.18}$$

The values for the signals strengths are given in Table 4.1 and were taken from Figure 5 of Reference [29]. The other type of constraints from the LHC data are the bounds on other neutral and charged

Decay Mode	Production Processes			
	ggF	VBF	VH	ttH
$H \to \gamma\gamma$	$0.96^{+0.14}_{-0.14}$	$1.39^{+0.40}_{-0.35}$	$1.09^{+0.58}_{-0.54}$	$1.10^{+0.41}_{-0.35}$
$H \to ZZ$	$1.04^{+0.16}_{-0.15}$	$2.68^{+0.98}_{-0.83}$	$0.68^{+1.20}_{-0.78}$	$1.50^{+0.59}_{-0.57}$
$H \to WW$	$1.08^{+0.19}_{-0.19}$	$0.59^{+0.36}_{-0.35}$	–	$1.50^{+0.59}_{-0.57}$
$H \to \tau\tau$	$0.96^{+0.59}_{-0.52}$	$1.16^{+0.58}_{-0.53}$	–	$1.38^{+1.13}_{-0.96}$
$H \to bb$	–	$3.01^{+1.67}_{-1.61}$	$1.19^{+0.27}_{-0.25}$	$0.79^{+0.60}_{-0.59}$

Table 4.1: Values for μ_{ij} taken from [29]

scalars. This we implemented using the most recent version of `HiggBounds5` [30].

4.1.3 Constraints from BR($B \to X_s\gamma$)

In models with charged scalar bosons, it is well known [31, 17, 18, 32, 33] that the experimental limits on the BR($B \to X_s\gamma$) can put important constraints in the parameter space of these models. For instance, in Reference [18] the bound

$$m_{H^+} > 580\,\mathrm{GeV}\,, \tag{4.19}$$

is derived for the type 2 2HDM at 95% CL (2σ). In fact the exact number depends on the errors both in the theoretical calculation [34] as well as in the experimental errors. For instance, the result for the SM at NNLO is [35, 33]

$$\mathrm{BR}^{\rm SM}(B \to X_s\gamma) = (3.40 \pm 0.17) \times 10^{-4}\,, \tag{4.20}$$

which shows an error of 5%, to be compared with the world average [36]

$$\mathrm{BR}^{\rm exp}(B \to X_s\gamma) = (3.32 \pm 0.15) \times 10^{-4}\,. \tag{4.21}$$

Here we take the approach of considering for the theoretical error a band around the central value of the calculation with an error of 2.5%, and following [33], for the experimental error, we consider 99%CL (3σ), that is,

$$2.78 \times 10^{-4} < \mathrm{BR}(B \to X_s\gamma) < 3.77 \times 10^{-4}\,. \tag{4.22}$$

The calculation

Our calculation follows closely the original calculation of Reference [17]. The central point in that calculation is that the new contributions from the charged scalar bosons are encoded in the Wilson coefficients,

$$C_7^{0,\text{eff}}(\mu_W) = C_{7,\text{SM}}^{0,\text{eff}}(\mu_W) + |Y|^2 C_{7,\text{YY}}^{0,\text{eff}}(\mu_W) + (XY^*) C_{7,\text{XY}}^{0,\text{eff}}(\mu_W)\,, \tag{4.23a}$$

$$C_8^{0,\text{eff}}(\mu_W) = C_{8,\text{SM}}^{0,\text{eff}}(\mu_W) + |Y|^2 C_{8,\text{YY}}^{0,\text{eff}}(\mu_W) + (XY^*) C_{8,\text{XY}}^{0,\text{eff}}(\mu_W)\,, \tag{4.23b}$$

$$C_4^{1,\text{eff}}(\mu_W) = E_0(x) + \frac{2}{3}\log\left(\frac{\mu_W^2}{M_W^2}\right) + |Y|^2 E_H(y)\,, \tag{4.23c}$$

$$C_7^{1,\text{eff}}(\mu_W) = C_{7,\text{SM}}^{1,\text{eff}}(\mu_W) + |Y|^2 C_{7,\text{YY}}^{1,\text{eff}}(\mu_W) + (XY^*) C_{7,\text{XY}}^{1,\text{eff}}(\mu_W)\,, \tag{4.23d}$$

$$C_8^{1,\text{eff}}(\mu_W) = C_{8,\text{SM}}^{1,\text{eff}}(\mu_W) + |Y|^2 C_{8,\text{YY}}^{1,\text{eff}}(\mu_W) + (XY^*) C_{8,\text{XY}}^{1,\text{eff}}(\mu_W)\,. \tag{4.23e}$$

All the expressions needed are given in Reference [17]. Also there one finds the way to evolve these coefficients to the scale $\mu_b = m_b$. The dependence on the charged scalar mass appears because the functions, $C_{i,\text{YY}}^{0,\text{eff}}, C_{i,\text{XY}}^{0,\text{eff}}, C_{i,\text{YY}}^{1,\text{eff}}, C_{i,\text{XY}}^{1,\text{eff}}$, depend on $y = m_t^2/m_{H^+}^2$ while the SM coefficients depend on $x = m_t^2/M_W^2$.

The generalization for models with more charged scalars is straightforward. The case of two charged scalar bosons was considered in Reference [33]. We just give the example of $C_7^{1,\text{eff}}(\mu_W)$, all the other having similar expressions.

$$\begin{aligned} C_7^{1,\text{eff}}(\mu_W) =& C_{7,\text{SM}}^{1,\text{eff}}(\mu_W) + |Y_1|^2 C_{7,\text{YY}}^{1,\text{eff}}(\mu_W, y_1) + |Y_2|^2 C_{7,\text{YY}}^{1,\text{eff}}(\mu_W, y_2) \\ &+ (X_1 Y_1^*) C_{7,\text{XY}}^{1,\text{eff}}(\mu_W, y_1) + (X_2 Y_2^*) C_{7,\text{XY}}^{1,\text{eff}}(\mu_W, y_2)\,, \end{aligned} \tag{4.24}$$

where X_i, Y_i are defined in Equation (A.6), taking the values in Equation (A.7a) for Zee-type models, and we wrote explicitly the dependence on the charged scalar masses,

$$y_1 = \frac{m_t^2}{m_{H_1^+}^2}, \quad y_2 = \frac{m_t^2}{m_{H_2^+}^2}\,. \tag{4.25}$$

An important point in the calculation is the value of the input parameters. We took those of Reference [17] except for $\alpha_s(M_Z)$, m_t, M_Z, M_W that were updated to the values of the PDG [37]. The values are

$$\alpha_s(M_Z) = 0.1179 \pm 0.0010, \qquad m_t = 172.76 \pm 0.3\,\text{GeV}\,, \tag{4.26a}$$

$$m_c/m_b = 0.29 \pm 0.02 \qquad m_b - m_c = 3.39 \pm 0.04\,\text{GeV}\,, \tag{4.26b}$$

$$\alpha_{em}^{-1} = 137.036\pm \qquad |V_{ts}^* V_{tb}/V_{cb}|^2 = 0.95 \pm 0.03\,, \tag{4.26c}$$

$$\text{BR}_{SL} = 0.1049 \pm 0.0046\,. \tag{4.26d}$$

We should emphasize that, using the input values of Reference [17], we were able to reproduce their results[2] for the SM.

[2]We are indebted to C. Greub for discussions and for having shared with us the original code for cross checking our independent calculation. One important point was that the parameter $\lambda_1 = 0.12$ GeV^2 defined in Reference [17] should be positive.

The result for the 2HDM type 2

First we considered the particular case of the 2HDM with type 2 couplings to fermions. In our model this is accomplished by setting $\gamma = 0$. Then the second Higgs decouples completely ($X_2 = Y_2 = 0$) and we have an effective 2HDM. The results are shown in Figure 4.1. On the left panel we considered a band

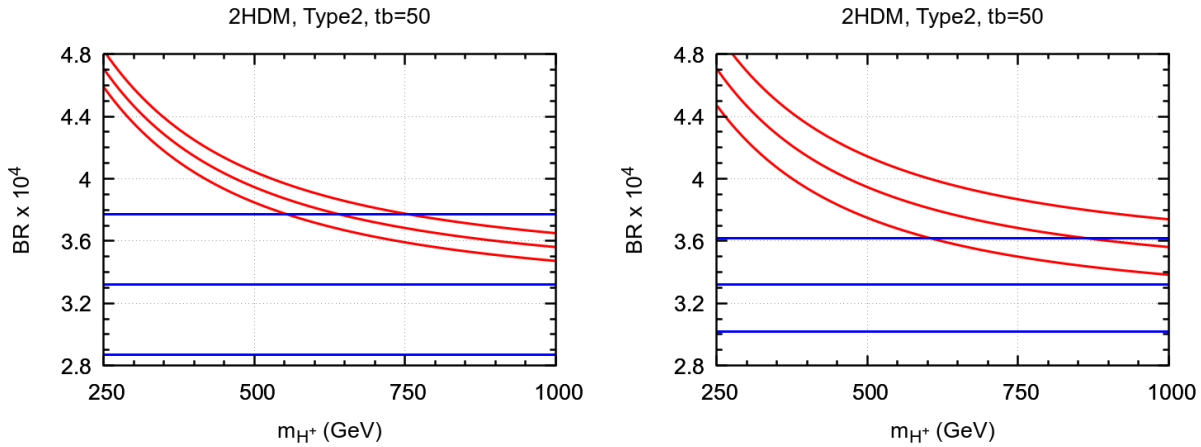

Figure 4.1: BR($B \to X_s\gamma$) as a function of the charged scalar mass. Left panel: The lines in blue represent the 3σ experimental limits, and those in red to 2.5% error in the calculation. Right panel: The lines in blue represent the 2σ experimental limits, and those in red to 5% error in the calculation.

corresponding to 2.5% in the calculation and a 3σ band for the experimental result. On the right panel we considered a band corresponding to 5% in the calculation and a 2σ band for the experimental result. We see that the limit for the mass of the charged scalar that we get is similar in both cases and also similar to what was obtained in Reference [18]

As we are not doing a NNLO calculation, our goal here is not to improve the limit for the 2HDM with type 2 couplings. We just want to show that in models with more charged scalars, as was addressed in Reference [33], the limit in Equation (4.19) can be relaxed for one of them and this will have implications for Zee-type models. We discuss this in the next section for the case of Zee-type models. For definiteness we take the choice on the left panel of Figure 4.1.

Implications for Zee-type Models

We have just seen that in the case of having just one charged scalar boson we have a limit for its mass coming from the BR($B \to X_s\gamma$) for the case of 2HDM with type 2 fermion couplings. Now we consider the case of Zee-type models also with type 2 fermion couplings. We start by just considering the variation of the masses and of the mixing angle γ without imposing all the theoretical and experimental constraints on the model. That will be done below when we consider the discussion of benchmark points. Our purpose here is just to show how the constraints from BR($B \to X_s\gamma$) can be satisfied in the model. Although we can always choose $m_{H_1^+} < m_{H_2^+}$, we start by not imposing that constraint. All points satisfying Equation (4.22) are shown on the left panel of Figure 4.2. We see that we have an exclusion for both masses to be below the value found (in the 2HDM) with one single charged scalar, but it is possible that one of the

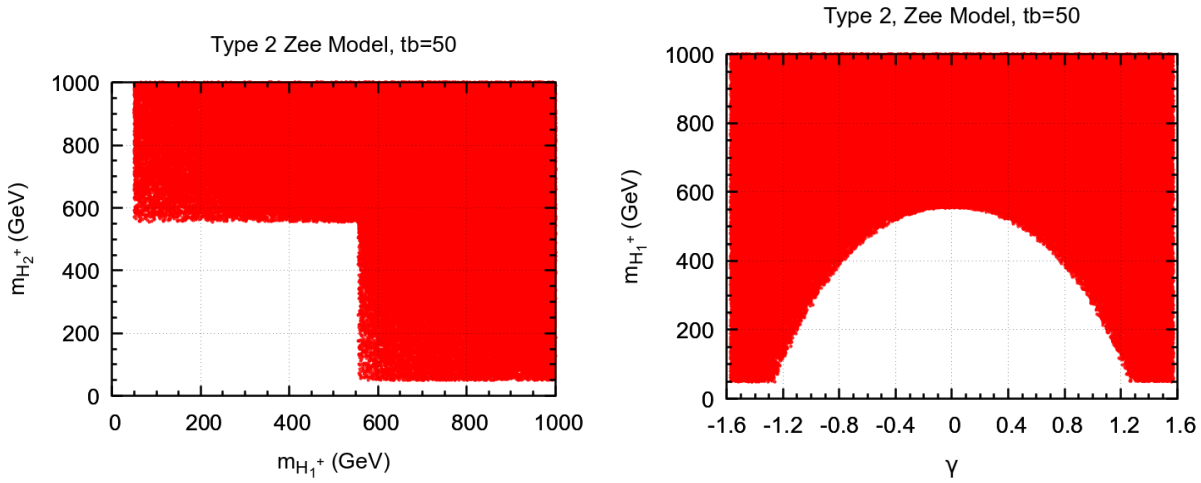

Figure 4.2: Left panel: points satisfying Equation (4.22) for Zee-type models. Right panel: mass of the lightest charged scalar boson as a function of the mixing angle γ.

masses is lower than 580 GeV if the other is above. This is a function of the mixing angle γ, as shown on the right panel of Figure 4.2. We see that $m_{H_1^+}$ can be as low as 50 GeV if the mixing angle is close to $\pm\pi/2$. Notice that for $\gamma = 0$ we recover the previous result. As can be seen from Figure 4.2, when $m_{H_1^+}$ is low, the other mass has always to be above the 580 GeV limit.

This result means that for each point in parameter space we have to evaluate the BR($B \to X_s\gamma$) to see if it passes the bounds in Equation (4.22), instead of using just one fixed limit for all points, like in the 2HDM.

There is a final comment. The charged Higgs contribute to $\Delta M_{B_{s,d}}$, coming from the B meson oscillations. We have not considered this contribution from flavour data because, as shown in [38], they are important only for very low $\tan\beta$, below what we already exclude from the other constraints; see Figure 4.3 below.

4.1.4 Scanning strategy

We made our scans varying the parameters in the following ranges,

$$m_{h_1} = 125\,\text{GeV}, \qquad m_{h_2}, m_{h_3}, m_{H_1^+} \in [100, 1000]\text{GeV}, \qquad m_{H_2^+} \in [500, 1000]\text{GeV}, \tag{4.27}$$

$$\alpha \in [-\frac{\pi}{2}, \frac{\pi}{2}], \qquad \tan\beta \in [0, 60], \qquad \gamma \in [-\frac{\pi}{2}, \frac{\pi}{2}], \tag{4.28}$$

$$m_{12}^2 \in [10^{-1}, 10^6]\text{GeV}^2, \qquad \lambda_c \in [10^{-3}, 10^2], \qquad k_1 \in [10^{-3}, 10^2], \tag{4.29}$$

$$k_2 \in [10^{-3}, 10^2], \qquad k_{12} \in [10^{-3}, 10^2], \tag{4.30}$$

and take randomly m_{12}^2, k_{12} with both signs. Despite this flat scan, there are large correlations in the points that satisfy all the constraints. For instance, we show in Figure 4.3 the correlation between α and β. We see that all the points satisfy $|\cos(\beta - \alpha)| \lesssim 1$, that is they are close to the alignment limit, where the 125GeV neutral scalar has couplings equal to their SM values. The points with negative α

correspond to the wrong sign of the fermion couplings [39, 40]. We also see that despite having varied $\tan\beta$ in a larger interval, the good points have $\tan\beta \in [1, 10]$.

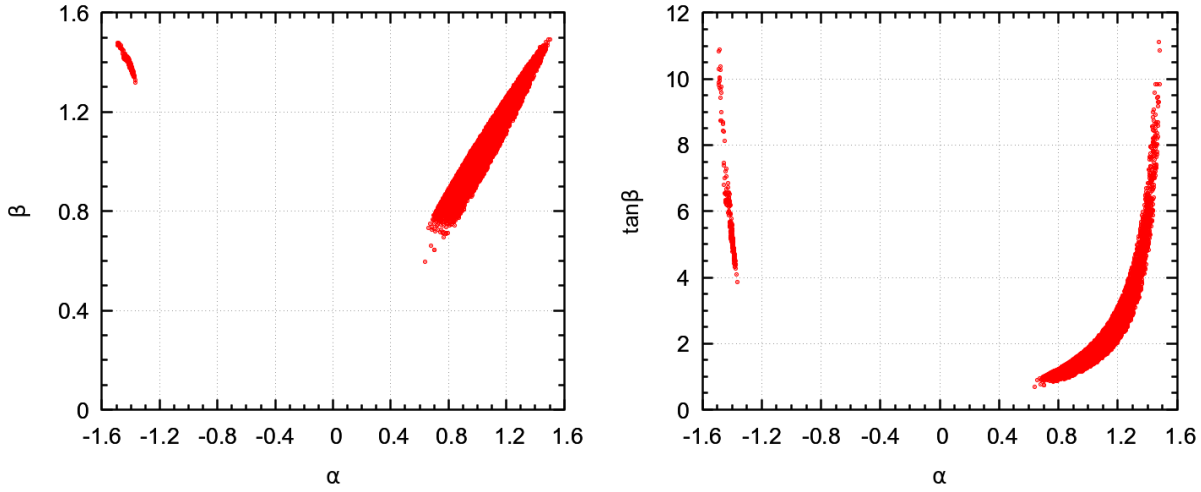

Figure 4.3: Left panel: correlation between α and β; Right panel: correlation between α and $\tan\beta$.

4.2 Impact of the charged scalars on the decays $h \to \gamma\gamma$ and $h \to Z\gamma$

4.2.1 The diagrams of the charged scalars

As we discussed before, the distinctive feature of our implementation of Zee-type models is the appearance of the off-diagonal coupling $ZH_1^{\pm}H_2^{\mp}$. This contributes to the loop decay $h \to Z\gamma$ and, in principle, could lead to some new feature. For the decay $h \to \gamma\gamma$, on the contrary, because of the photon coupling being always diagonal, the contribution of the charged scalars will not depend on the off-diagonal $ZH_1^{\pm}H_2^{\mp}$ coupling. In fact, the diagrams coming from the charged scalars and contributing in this model for $h \to \gamma\gamma$ are shown in Figure 4.4 while for the case of the decay $h \to Z\gamma$, besides those equivalent to Figure 4.4 (with one γ exchanged with a Z) we also have those with the off-diagonal coupling, as shown in Figure 4.5. The formulas for these loop decays in the absence of couplings of the type $ZH_1^+H_2^+$ are well known. They were explicitly written for the C2HDM in Reference [41] and, for $h \to \gamma\gamma$, they can be easily adapted for the case of Zee-type models. We generalize the formulas for $h \to Z\gamma$ to include the new couplings, and write the full expressions in Appendix B.

4.2.2 Discussion of the impact of the charged scalars on the loop decays

Couplings $h_1H_j^+H_k^-$

The couplings $h_1H_1^+H_1^-$ and $h_1H_2^+H_2^-$ do not have a strong dependence on γ. On the contrary the couplings $h_1H_1^+H_2^-$ and $h_1H_2^+H_1^-$ are proportional to $\sin\gamma$.

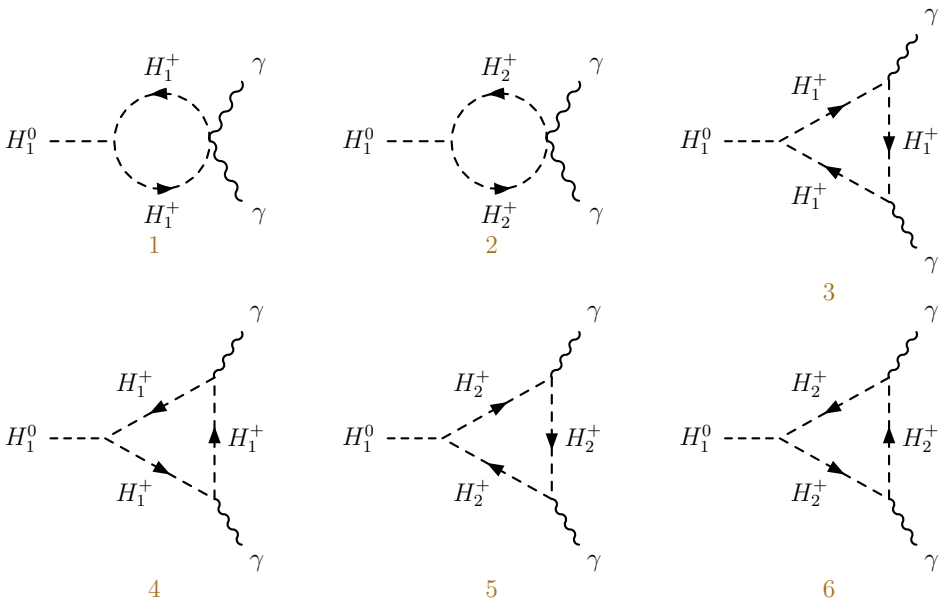

Figure 4.4: Charged scalars contributions to $h \to \gamma\gamma$

Couplings $ZH_j^+H_k^-$

The couplings $ZH_1^+H_2^-$ and $ZH_2^+H_1^-$ are given in Equations (A.2b)-(A.2c). They are proportional to $\sin(2\gamma)$ and vanish for $\gamma = 0, \pm\pi/2$, while the couplings $ZH_1^+H_1^-$ and $ZH_2^+H_2^-$ vary with γ like

$$g_{ZH_i^+H_i^-} \propto (-1 + 4s_W^2 + \cos 2\gamma)\,. \tag{4.31}$$

It is interesting to note that because $-1 + 4s_W^2 \simeq 0$ they behave approximately like $\cos 2\gamma$ that vanishes at $\pm\pi/4$.

Results and Conclusions

Because of the dependence of the couplings on the mixing angle γ, we looked at the contributions of the charged scalars as a function of this angle. If the loop integral did not vary much with the masses, the results would be proportional to the products of the $h_1H_j^+H_k^-$ and $ZH_j^+H_k^-$ couplings, as the photon coupling is universal. In the following figures all points passed all the constraints, including HiggsBounds 5.9.1 and those coming from BR($B \to X_s\gamma$), as discussed in section 4.1.3.

In Figure 4.6 we show on the left panel the result of the product of the couplings (we divide by v because the coupling $h_1H_j^+H_k^-$ has dimensions of mass), first for the the case of H_1^+ running in the loops of Figure 4.4 in red and then for the case of H_2^+ in blue. From the above discussion we expect the result to vary like $\cos 2\gamma$, and that is indeed the case. Our assumptions that the loop integrals do not depend much on the masses can be verified in the right panel of Figure 4.6 where we show the actual plot for the loop amplitudes. The behaviour as $\cos 2\gamma$ is clear in both cases.

Now we can study the case where there are two different charged scalars, H_1^+ and H_2^+, running in the loops of Figure 4.5. This is shown in Figure 4.7. Again on the left panel we plot the product of the couplings, and on the right panel the loop amplitudes. In this case Amp(H_1^+, H_2^+), corresponding to

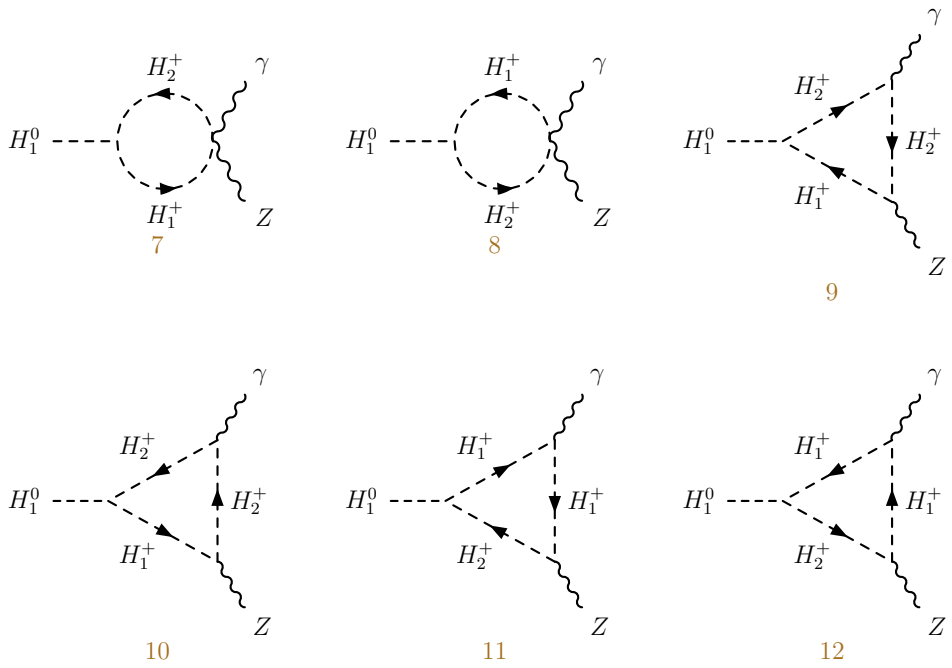

Figure 4.5: Extra charged scalars contributions to $h \to Z\gamma$

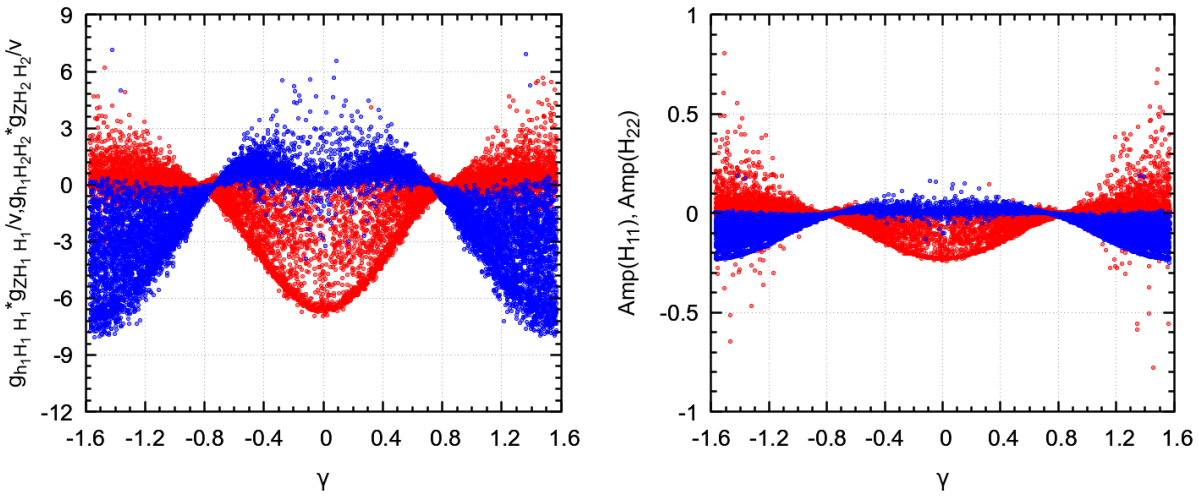

Figure 4.6: Results for the charged scalars amplitudes contribution to $h \to Z\gamma$. On the left panel the coupling products and on the right panel the actual amplitudes.

diagrams 7, 10 and 11 of Figure 4.5 in red, coincides with Amp(H_2^+, H_1^+) corresponding to diagrams 8, 9 and 12. As expected we see clearly a dependence on $\sin 2\gamma$, confirming our expectations.

However this nice result will not help us in using the decay $h \to Z\gamma$ to identify the novel coupling $ZH_1^+H_2^-$ appearing in Zee-type models. The problem is that once we sum all contributions we loose the dependence on γ. This can be seen on Figure 4.8 both for the products of the couplings in the left panel, and for the final result for the charged scalar contribution to $h \to Z\gamma$.

In conclusion, although the contribution of the charged scalars can have both signs and also be zero, the dependence on γ and therefore on the mixing parameters μ_4 is hidden. In fact we can have the same behaviour of the charged scalar amplitudes in other models like the 3HDM [42].

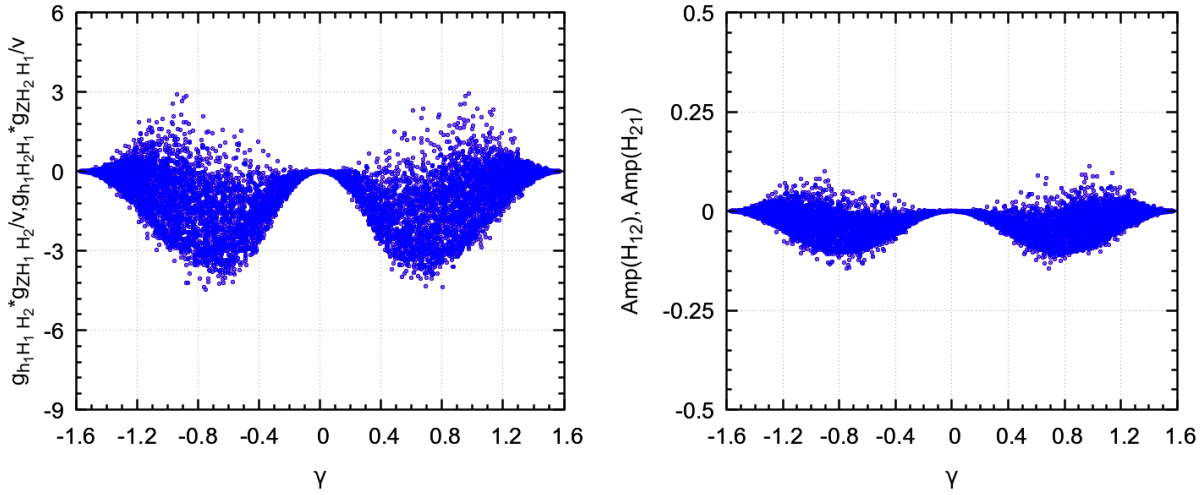

Figure 4.7: Results for the charged scalars amplitudes contribution to $h \to Z\gamma$. On the left panel the coupling products and on the right panel the actual amplitudes.

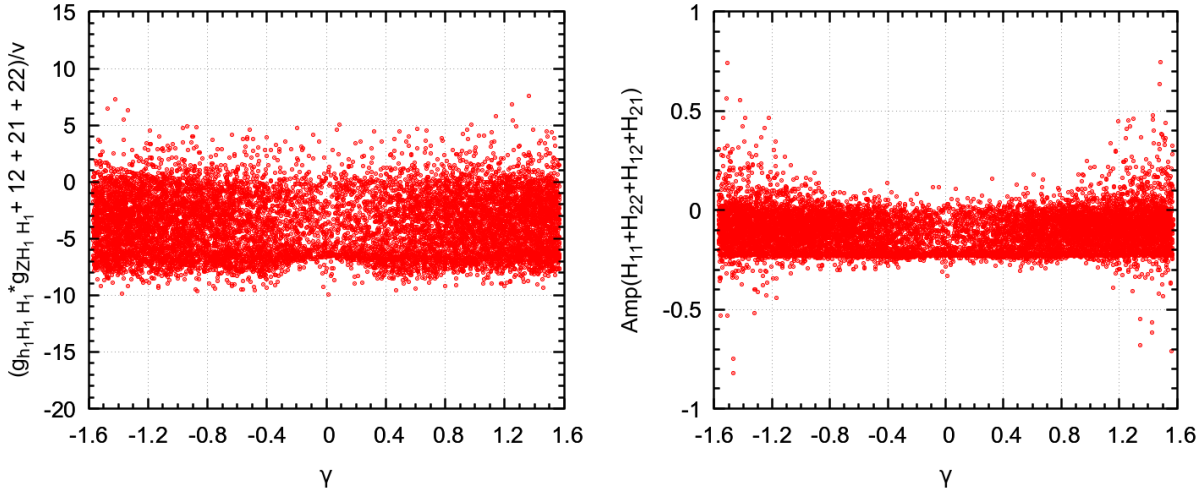

Figure 4.8: Results for the charged scalar amplitudes contribution to $h \to Z\gamma$. On the left panel the sum of the product of couplings and on the right panel the complete result.

4.3 Decays of the Charged Higgs

4.3.1 The decay $H_2^+ \to H_1^+ + Z$

If we want to have a unique signal for this model it would be the decay of one charged Higgs in another one plus a Z boson. This is only possible if $\gamma \neq 0$. We have checked that this can indeed occur, as shown in Figure 4.9. All points shown satisfy all the constraints discussed in Section 4.1. We see clearly that, as expected, one has to be away from $\gamma = 0$ to have a sizable decay width.

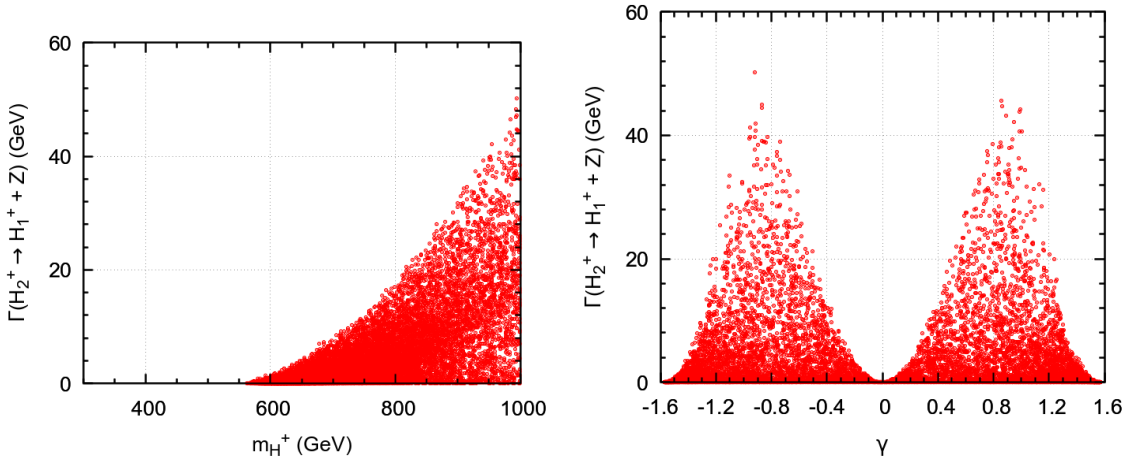

Figure 4.9: Decay with $H_2^+ \to H_1^+ + Z$. On the left panel the dependence on the mass of the decaying charged Higgs and on the right the dependence on γ.

Decays of the heavier $H_2^\pm$

Depending on the masses the following decays are among the most important,

$$H_2^\pm \to H_1^\pm + Z\,, \qquad H_2^+ \to t + \overline{b}\,, \qquad H_2^\pm \to H_1^\pm + h_i\,, \tag{4.32}$$

$$H_2^\pm \to W^\pm + h_i\,, \qquad H_2^+ \to \nu_\tau + \tau^+\,. \tag{4.33}$$

The first decay is unique to this type of models and not present in NHDM. It requires a mixing between the charged Higgs from the doublets with the charged Higgs from the singlets. The expression for the width is

$$\Gamma(H_2^\pm \to H_1^\pm + Z) = \frac{g^2}{64\pi m_{H_j^+}^3 M_W^2}\, g_{\mathrm{HpjHmkZ}}[2,1]^2\, \lambda(m_{H_2^+}^2, m_{H_1^+}^2, M_Z^2)^3, \tag{4.34}$$

where the Källen function is given by

$$\lambda(x^2, y^2, z^2) = \sqrt{x^4 + y^4 + z^4 - 2x^2y^2 - 2x^2z^2 - 2y^2z^2}. \tag{4.35}$$

and $g_{\mathrm{HpjHmkZ}}[2,1]$ is given in Equation (A.2c).

For the other decays we have

$$\Gamma(H_2^+ \to t + \overline{b}) = \frac{3g^2}{32\pi M_W^2} m_{H_2^+} \lambda(m_{H_2^+}, m_t^2, m_b^2)\left[(1 - x_t - x_b)(Y_2^2 x_t + X_2^2 x_b) - 4x_t x_b X_2 Y_2\right], \tag{4.36}$$

where

$$x_t = \frac{m_t^2}{m_{H_2^+}}, \quad x_b = \frac{m_b^2}{m_{H_2^+}}, \tag{4.37}$$

and X_k, Y_k are given in Equation (A.7a). For the decay into the other charged Higgs and one neutral Higgs boson we have,

$$\Gamma(H_2^\pm \to H_1^\pm + h_i) = \frac{g_{\mathrm{hjHpiHmk}}[i,2,1]^2}{16\pi m_{H_2^+}^3} \lambda(m_{H_2^+}, m_{H_1^+}, m_{h_i}^2). \tag{4.38}$$

where $g_{\mathrm{hjHpiHmk}}[i,2,1]$ is given in Equation (A.8).

The decay into one W and one neutral Higgs boson is similar to the decay into the charged Higgs and Z. We obtain

$$\Gamma(H_2^\pm \to W^\pm + h_i) = \frac{g^2}{64\pi m_{H_2^+}^3 M_W^2}\, g_{\mathrm{hjHpkWm}}[i,2]^2\, \lambda(m_{H_2^+}^2, M_W^2, m_{h_i}^2)^3. \tag{4.39}$$

where $g_{\mathrm{hjHpkWm}}[i,2]$ is given in Equations (A.5b) (A.5d) and (A.5f).

Finally the decay in the third family leptons (the others are negligible) is given by

$$\Gamma(H_2^+ \to \nu_\tau + \tau^+) = \frac{g^2}{32\pi M_W^2}\, Z_2^2\, m_\tau^2\, m_{H_2^+} \left[1 - \frac{m_\tau^2}{m_{H_2^+}^2}\right]^2. \tag{4.40}$$

Decays of the lighter $H_1^\pm$

Except for the decays into another charged Higgs, that are not allowed because we assume that $m_{H_1^+} < m_{H_2^+}$, the decays are similar to those of the heavier charged scalar. If kinematically available, the expressions for the decays can be easily obtained from the above with index $2 \to 1$.

4.4 Benchmark points for Zee-type models

4.4.1 Looking for a distinctive signature

As we have discussed before, Zee-type models provide an example of the non-vanishing coupling between two different charged Higgs and the Z boson. For instance, this cannot happen in any NHDM, even with a large N. So we want to see if there is a signal of this coupling.

As we explained in section 4.2, the first idea was to look at the impact on the BR($h_{125} \to Z\gamma$). But it turns out that the effect of the extra diagrams is not quantitatively different from the effect of a second charged scalar coupling only diagonally to the Z boson, as occurs for instance in the 3HDM, where there are two charged Higgs bosons, but no $ZH_1^+H_2^-$ coupling [42]. So, although there is an effect, for instance the contribution of summing over all the charged Higgs diagrams can vanish, this is not an effect specific to the $ZH_1^+H_2^-$ coupling. So we turn to a distinctive decay:

$$H_2^+ \to H_1^+ + Z, \quad \text{and} \quad H_1^+ \to t + \bar{b}\,. \tag{4.41}$$

This decay has a very clear signature and should be searched for at the LHC.

4.4.2 Benchmark Point P_1

As the model has many independent parameters, if we try to plot the various branching ratios of the H_1^+ or H_2^+ instead of obtaining something similar to the famous plot [43] of the SM Higgs boson BR's as a function of its mass (when this mass was yet not known), we would get a figure with all the points

superimposed and no lines. So, to have a better visualization we fix most of the parameters and show that indeed the branching ratios for the processes in Equation (4.41) can be important, or even dominant. This leads us to the choice of benchmark points. In choosing these benchmark points for Zee-type models we take in account all the theoretical and experimental constraints on the model. Then, we scan the parameters around the benchmark points, so that one can visualise the whole benchmark region.

For the first benchmark point, P_1, we choose a situation when both masses are above[3] the limit of Equation (4.19). It is defined by the following parameters,

$$m_{h_1} = 125\,\text{GeV} \qquad m_{h_2} = 714.98\,\text{GeV} \qquad m_{h_3} = 767.42\,\text{GeV} \tag{4.42a}$$

$$m_{H_1^+} = m_{H_2^+} - 200\,\text{GeV} \qquad \alpha = 1.391 \qquad \gamma = 0.894 \tag{4.42b}$$

$$m_{12}^2 = 8.828 \times 10^4\,\text{GeV}^2 \qquad \lambda_c = 0.4363 \qquad k_1 = 0.4633 \tag{4.42c}$$

$$k_2 = 0.4633 \qquad k_{12} = 5.427 \times 10^{-2} \tag{4.42d}$$

The situation is shown in Figure 4.10. We see that our signal decay has the largest branching ratio,

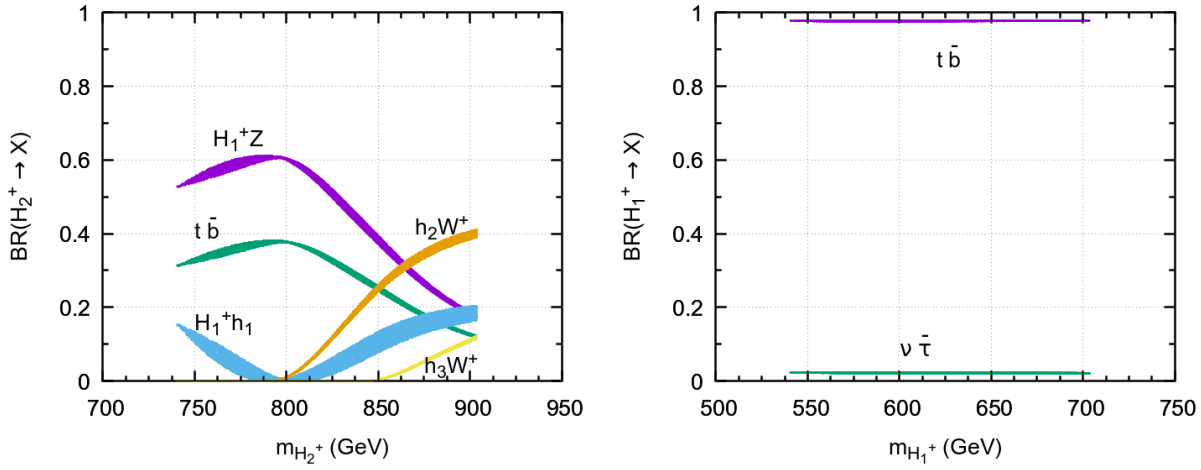

Figure 4.10: Dominant BR's for H_2^+ (left panel) and H_1^+ (right panel) for benchmark point P_1.

while H_1^+ decays almost 100% into $t + \bar{b}$. This should provide clear signatures at the LHC. A detailed analysis, with background studies, should of course be done. The width of the bands comes from the variation of $\tan\beta$ (at the percent level, because the good points have $\alpha \simeq \beta$). All the points pass all the constraints, including that of Equation (4.22).

4.4.3 Benchmark Point P_2

One could argue that P_1 will lead to a situation where the constraint of Equation (4.22) was verified, as we took the masses to satisfy the bound of Equation (4.19). Therefore we want to show another benchmark point that would be excluded by Equation (4.19). That is, we do not exclude points *a priori*, but for each point we evaluate the BR($B \to X_s\gamma$) to see if it passes the bounds in Equation (4.22).

[3] The starting point satisfied Equation (4.19), but as we vary the masses some points are slightly below that limit.

For the second benchmark point P_2 we therefore choose a situation where the lowest charged Higgs mass is below that limit. It is defined by the following parameters

$$m_{h_1} = 125\,\text{GeV} \qquad m_{h_2} = 580.7\,\text{GeV} \qquad m_{h_3} = 633.7\,\text{GeV} \tag{4.43a}$$

$$m_{H_1^+}, m_{H_2^+}\text{GeV, scanned as shown} \qquad \alpha = 1.398 \qquad \gamma = 1.089 \tag{4.43b}$$

$$m_{12}^2 = 5.77 \times 10^4\,\text{GeV}^2 \qquad \lambda_c = 4.473 \qquad k_1 = 1.082 \tag{4.43c}$$

$$k_2 = 3.98 \times 10^{-3} \qquad k_{12} = -1.266 \times 10^{-3} \tag{4.43d}$$

The situation is shown in Figure 4.11. We see that our signal decay has the largest branching ratio, while

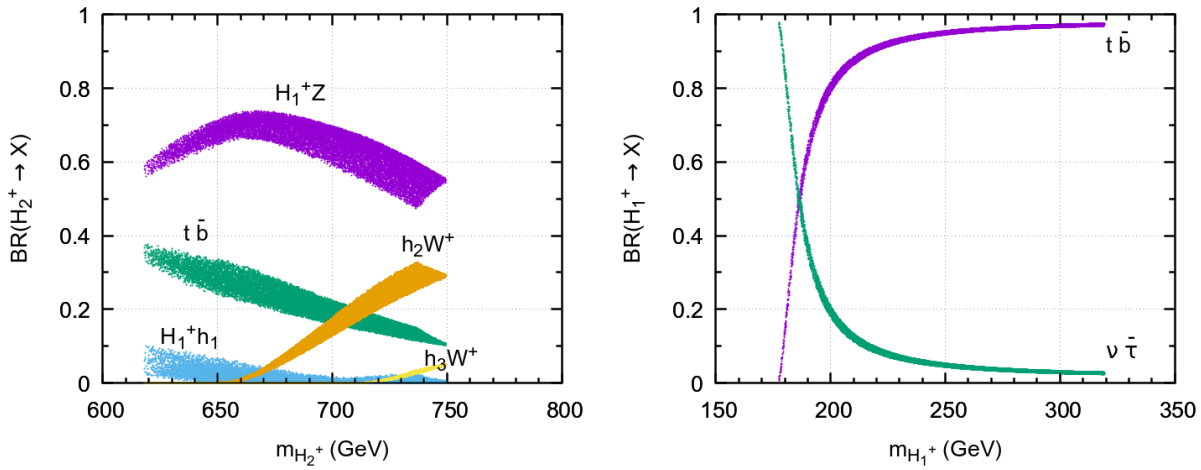

Figure 4.11: Dominant BR's for H_2^+ (left panel) and H_1^+ (right panel) for benchmark point P_2.

H_1^+ decays almost 100% into $t + \bar{b}$. This should be clear signatures at the LHC, although background studies should be done. The width of the bands comes from the variation of $\tan\beta$ and $m_{H_1^+}, m_{H_2^+}$ which were varied independently. All the points pass all the constraints, including that of Equation (4.22).

4.4.4 Benchmark Point P_3

We have a large set of benchmark points that illustrate our signal, the decay $H_2^+ \to H_1^+ + Z$. We just give another example, our benchmark point P_3. It is defined by the following parameters,

$$m_{h_1} = 125\,\text{GeV} \qquad m_{h_2} = 728.3\,\text{GeV} \qquad m_{h_3} = 720.5\,\text{GeV} \tag{4.44a}$$

$$m_{H_1^+}, m_{H_2^+}\text{GeV, scanned as shown} \qquad \alpha = 1.401 \qquad \gamma = -1.145 \tag{4.44b}$$

$$m_{12}^2 = 9.48 \times 10^4\,\text{GeV}^2 \qquad \lambda_c = 2.67 \times 10^{-2} \qquad k_1 = 7.149 \tag{4.44c}$$

$$k_2 = 1.425 \times 10^{-2} \qquad k_{12} = 1.29 \times 10^{-2} \tag{4.44d}$$

The situation is shown in Figure 4.12. Again we see that our signal decay has the largest branching ratio, while H_1^+ decays almost 100% into $t + \bar{b}$. The width of the bands comes from the variation of $\tan\beta$ and $m_{H_1^+}, m_{H_2^+}$ which were varied independently. All the points pass all the constraints, including that of

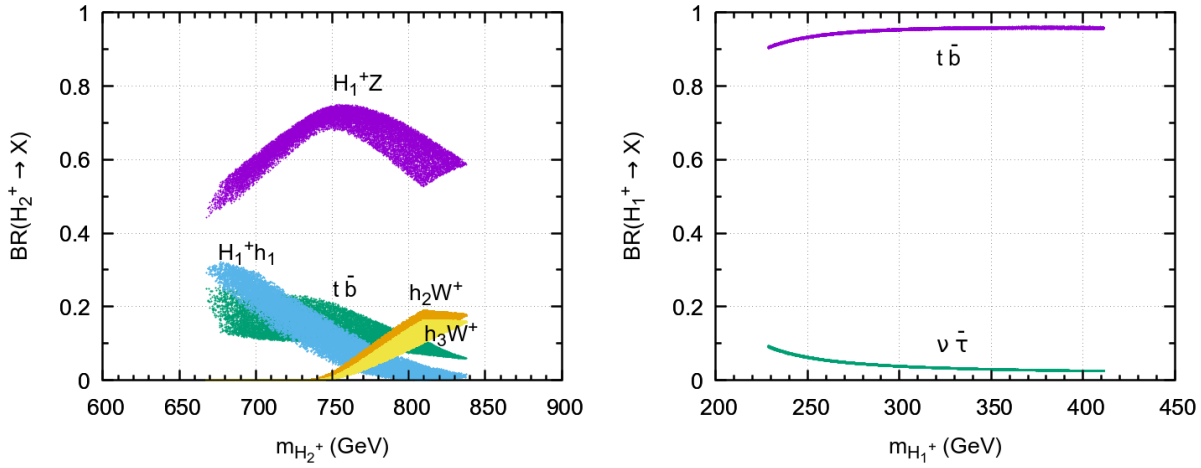

Figure 4.12: Dominant BR's for H_2^+ (left panel) and H_1^+ (right panel) for benchmark point P_3.

Equation (4.22).

4.4.5 Benchmark Point P_4

It has been pointed out recently [44], that there are some decay channels for the charged Higgs that have not been investigated at LHC. One of them is the decay $H_1^+ \to W^+ + h_1$. We looked in our data sample for points where the BR($H_1^+ \to W^+ + h_1$) could be large. For our model, after passing through the HiggsBounds 5, there are not many points of the general scan that have a large BR($H_1^+ \to W^+ + h_1$). We took one of these which is our benchmark point P_4. It is defined by the following parameters,

$$m_{h_1} = 125\,\text{GeV} \qquad m_{h_2} = 314.9\,\text{GeV} \qquad m_{h_3} = 651.3\,\text{GeV} \tag{4.45a}$$

$$m_{H_1^+},\, m_{H_2^+}\ \text{GeV, scanned as shown} \qquad \alpha = -1.402 \qquad \gamma = -1.421 \tag{4.45b}$$

$$m_{12}^2 = 1.85 \times 10^4\,\text{GeV}^2 \qquad \lambda_c = 2.00 \times 10^{-2} \qquad k_1 = 1.422 \times 10^{-2} \tag{4.45c}$$

$$k_2 = 0.432 \qquad k_{12} = -9.597 \times 10^{-3} \tag{4.45d}$$

The situation is shown in Figure 4.13. We see that, in our model, both BR($H_1^+ \to W^+ + h_1$) and BR($H_1^+ \to W^+ + h_2$) can be sizable. In this case, the BR($H_2^+ \to H_1^+ + Z$) is very small, around 2%. However the BR($H_2^+ \to W^+ + h_1$) and BR($H_2^+ \to W^+ + h_2$) can also be large, making this an interesting benchmark point. The width of the bands comes from the variation of $\tan\beta$, $m_{H_1^+}$, and $m_{H_2^+}$, which were varied independently. All the points pass all the constraints, including that of Equation (4.22).

4.4.6 Production cross-sections and Experimental bounds

One can ask if a charged Higgs boson with a large BR($H^+ \to t\bar{b}$) is not in contradiction with experimental bounds from the LHC. Although we have checked all the points with HiggsBounds 5.9.1 [30], it is perhaps helpful to show it explicitly for our benchmark points. The results are shown in Figure 4.14 and Figure 4.15. We used the values for the production cross-section $\sigma(pp \to tbH^+)$ from Reference [45, 46]. To

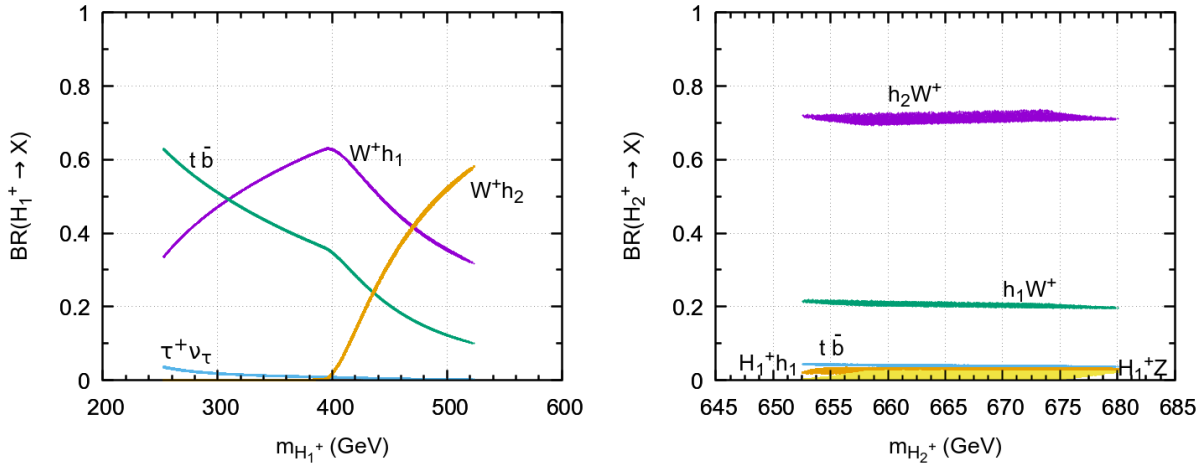

Figure 4.13: Dominant BR's for H_1^+ (left panel) and H_2^+ (right panel) for benchmark point P_4.

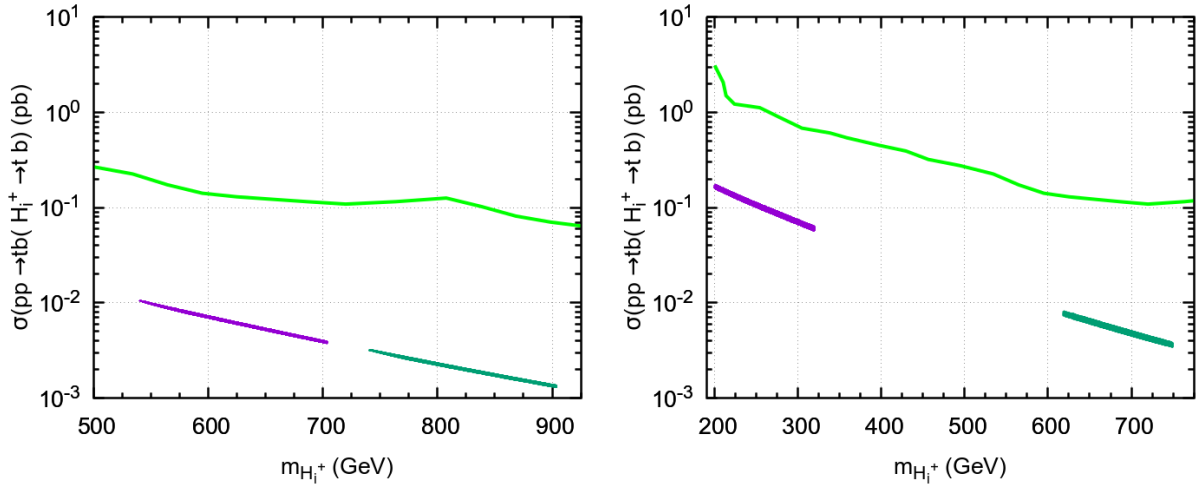

Figure 4.14: $\sigma(pp \to tbH^+) \times BR(H^+ \to tb)$ versus the charged Higgs mass for benchmark points P_1 (left panel) and P_2 (right panel). We took BR($H^+ \to tb$)$= 1$. The green line is the current LHC limit.

see if the points are allowed we considered the worst case scenario where BR($H^+ \to tb$)=1 (although for our benchmark points this is only true for the lightest charged Higgs boson); see Figure 4.7 and Figure 4.8. The green line is the current experimental bound from ATLAS [47] as discussed in Reference [44]. So we conclude that all our benchmark points are consistent with the latest LHC data.

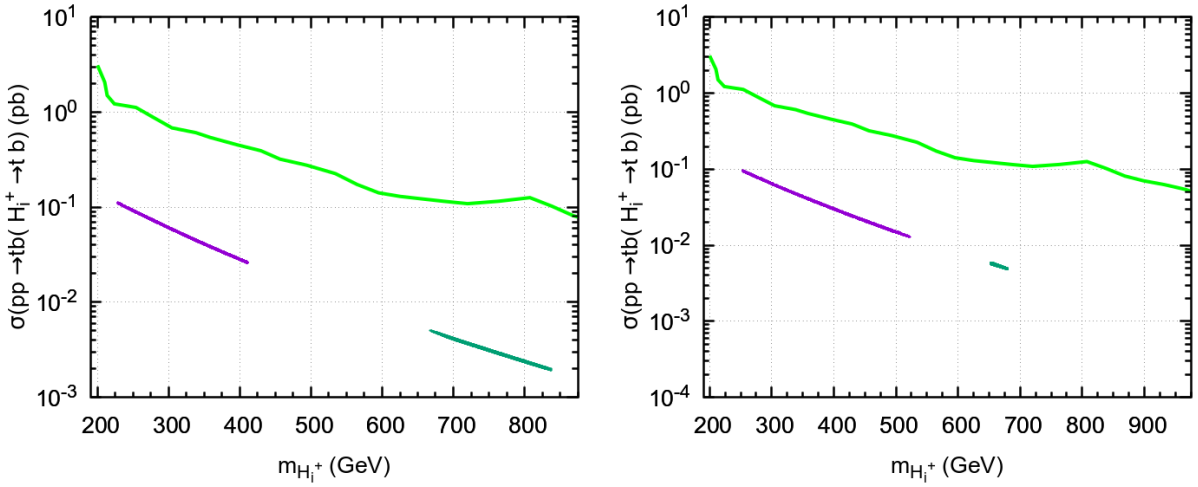

Figure 4.15: $\sigma(pp \to tbH^+) \times BR(H^+ \to tb)$ versus the charged Higgs mass for benchmark points P_1 (left panel) and P_2 (right panel). We took BR($H^+ \to tb$)$= 1$. The green line is the current LHC limit.

Chapter 5

Extra Gauge Symmetries

In this Chapter we extend some of the concepts studied in Chapters 2 and 3 to theories with additional gauge symmetries within the electroweak sector. We start by studying the Higgs mechanism for neutral gauge bosons in such theories, then we specialise to theories with the gauge group $SU(2) \times U(1) \times U(1)$ and study the rotation of the correspondent bosons to the physical basis, and finally we apply the formalism in the rest of the Chapter to a specific model with gauge group $SU(2) \times U(1) \times U(1)$ and a Higgs sector composed of a doublet and a higher multiplet.

5.1 Neutral Gauge Bosons

In a theory with a general electroweak gauge sector, and by ignoring all but the neutral gauge bosons, the covariant derivative can be written as

$$D^\mu = \partial^\mu + i \sum_{r=1}^{m} g_r Y_r X_r^\mu \,, \tag{5.1}$$

where X_r are the neutral gauge bosons, Y_r are the correspondent symmetry generators or hypercharges, and m is how many there are. The generators will have a variety of representations, and so will the scalars, but since, apart from a remaining $U(1)_{em}$, the symmetries are broken at our scales, we assume the vacua will appear in one specific entry of all their representations, such that

$$Y_r < \phi_i >= y_{ri} < \phi_i > \,. \tag{5.2}$$

We will assume there are n of those scalars, denote the entry of the vacuum by Φ_{iV}, and parameterize it as

$$\phi_{iv} = \frac{1}{\sqrt{2}}(v_i + h_i + i a_i) \,. \tag{5.3}$$

To study the physical spectrum, we calculate the covariant derivative acting on the vacuum entry and

keep only the terms we saw are relevant for the Higgs mechanism

$$D^{\mu}\phi_{iv} = \frac{i}{\sqrt{2}}\left(\partial^{\mu}a_i + \sum_{r}^{m} v_i g_r y_{ri} X_r^{\mu}\right) . \tag{5.4}$$

Proceeding to calculate the relevant part of the Lagrangian one finds

$$\mathcal{L}_{K0} = \sum_{i}^{n} |D^{\mu}\Phi_{iv}|^2 = \frac{1}{2}\sum_{i}^{n} \partial^{\mu}a_i \partial_{\mu}a_i + \sum_{ir}^{nm} v_i g_r y_{ri} X_r^{\mu}\partial_{\mu}a_i + \frac{1}{2}\sum_{irs}^{nmm} v_i^2 g_r g_s y_{ri} y_{si} X_r^{\mu} X_{s\mu} . \tag{5.5}$$

To write this last equation in a more useful notation, we define the following vectors

$$\bar{a} = \begin{pmatrix} \partial_{\mu}a_1 & \partial_{\mu}a_2 & . & . & \partial_{\mu}a_n \end{pmatrix}^T , \tag{5.6}$$

$$\bar{X} = \begin{pmatrix} X_1^{\mu} & X_2^{\mu} & . & . & X_m^{\mu} \end{pmatrix}^T , \tag{5.7}$$

$$\bar{c}_r = \begin{pmatrix} v_1 g_r y_{r1} & v_2 g_r y_{r2} & . & . & v_n g_r y_{rn} \end{pmatrix}^T , \tag{5.8}$$

and the following $n \times m$ matrix

$$C = \begin{pmatrix} \bar{c}_1 & \bar{c}_2 & . & . & \bar{c}_m \end{pmatrix} , \tag{5.9}$$

together with its $m \times m$ Graham Matrix

$$M^2 = C^T C = \begin{pmatrix} \bar{c}_1^T \\ \bar{c}_2^T \\ . \\ . \\ \bar{c}_m^T \end{pmatrix} \begin{pmatrix} \bar{c}_1 & \bar{c}_2 & . & . & \bar{c}_m \end{pmatrix} = \begin{pmatrix} \bar{c}_1 \cdot \bar{c}_1 & \bar{c}_1 \cdot \bar{c}_2 & . & . & \bar{c}_1 \cdot \bar{c}_m \\ \bar{c}_2 \cdot \bar{c}_1 & . & & & . \\ . & & . & & . \\ . & & & . & . \\ \bar{c}_m \cdot \bar{c}_1 & . & . & . & \bar{c}_m \cdot \bar{c}_m \end{pmatrix} . \tag{5.10}$$

Using these definitions

$$\mathcal{L}_{K0} = \frac{1}{2}\bar{a}^T\bar{a} + \bar{a}^T C\bar{X} + \frac{1}{2}\bar{X}^T M^2 \bar{X} . \tag{5.11}$$

Before applying the Higgs mechanism to obtain the physical fields, one needs to find the gauge bosons mass eigenstates by diagonalizing M^2. For that, we define the rotation matrix R such that

$$R M^2 R^T = M_D^2 , \tag{5.12}$$

where M_D^2 is the diagonal form of M^2. The mass eigenstates will then be

$$\bar{Y} = R\bar{X} , \tag{5.13}$$

and the matrix C can also be rotated as

$$C_D = CR^T\,, \tag{5.14}$$

so that M_D^2 is the Graham Matrix of C_D

$$M_D^2 = C_D^T C_D\,. \tag{5.15}$$

The Lagrangian then becomes

$$\mathcal{L}_{K0} = \frac{1}{2}\bar{a}^T\bar{a} + \bar{a}^T C_D \bar{Y} + \frac{1}{2}\bar{Y}^T M_D^2 \bar{Y}\,. \tag{5.16}$$

Since M_D^2 is diagonal, $\bar{v}_{Di}$, the column vectors of C_D, are all orthogonal. Their norm is the squared mass of the gauge bosons, and so, the vectors correspondent to massless gauge bosons, like the photon, will automatically be null vectors. One can then safely ignore the null columns of C_D and massless entries of M_D^2, turning those matrices into $k \times m$ and $k \times k$ respectively, where k in the number of massive gauge bosons. Using the vector $\bar{B}$ with k entries composed of only the massive gauge bosons of $\bar{Y}$,

$$\mathcal{L}_{K0} = \frac{1}{2}\bar{a}^T\bar{a} + \bar{a}^T C_D \bar{B} + \frac{1}{2}\bar{B}^T M_D^2 \bar{B}\,. \tag{5.17}$$

The Goldstone theorem guarantees that all massive gauge bosons have a correspondent Goldstone boson to absorb, meaning that $m \geq k$. Looking at 5.17, the goldstone coupled to each gauge boson is given by the columns of C_D, v_{Di}. If $m = k$, C_D is a square matrix. But, if $m > k$[1], that can be obtained by projecting the vectors v_{Di} to the k-dimensional space spanned by them. Denoting the $m \times k$ matrix that entails that projection by P, and the inverse operation by P^{-1} that satisfies $P^{-1}P = \mathbb{1}_{m\times m}$, we define

$$C_{DS} = PC_D\,, \tag{5.18}$$

$$\bar{b}^T = \bar{a}^T P^{-1}\,, \tag{5.19}$$

where now C_{DS} is $k \times k$, $\bar{b}$ has k entries, and $\bar{z}$ is composed by the $m - k$ scalar bosons not in $\bar{b}$.

The Lagrangian is then

$$\mathcal{L}_{K0} = \frac{1}{2}\bar{z}^T\bar{z} + \frac{1}{2}\bar{b}^T\bar{b} + \bar{b}^T C_{DS}\bar{B} + \frac{1}{2}\bar{B}^T M_D^2 \bar{B}\,, \tag{5.20}$$

and, after a little algebra, one finds

$$\mathcal{L}_{K0} = \frac{1}{2}\bar{z}^T\bar{z} + \frac{1}{2}\left(\bar{B}^T + \bar{b}^T(C_D^T)^{-1}\right) M_D^2 \left(\bar{B} + C_D^{-1}\bar{b}\right)\,. \tag{5.21}$$

Finally, using the gauge symmetry available for each entry of $\bar{B}$, one can redefine the gauge bosons

[1] Meaning that there are $m - k > 0$ massless neutra Gauge bosons.

to be

$$\bar{Z} = \bar{B} + C_D^{-1}\bar{b}\,, \tag{5.22}$$

leaving the Lagrangian as

$$\mathcal{L}_{K0} = \frac{1}{2}\bar{z}^T\bar{z} + \frac{1}{2}\bar{Z}^T M_D^2 \bar{Z}\,, \tag{5.23}$$

or, since the matrix M_D^2 is diagonal, and by denoting its eigenvalues m_i^2, this can be written simply as

$$\mathcal{L}_{K0} = \sum_i^{m-k} \frac{1}{2}\partial^\mu z_i \partial_\mu z_i + \sum_i^{k} \frac{1}{2} m_i^2 Z_i^\mu Z_{i\mu}\,, \tag{5.24}$$

where Z_i^μ are the physical massive gauge bosons.

5.2 $SU(2) \times U(1) \times U(1)$ Theories

In this section, we will look at the simplest example of just adding an additional $U(1)$ to the $SU(2) \times U(1)$ gauge symmetry used in previous chapters. The models with that property present us with the covariant derivative

$$D_\mu = \partial_\mu + igT_a W_\mu^a + ig_a Y_a X_{a\mu} + ig_b Y_b X_{b\mu}\,, \tag{5.25}$$

where we are mostly interested in the quantity

$$K_\mu^0 = gT_3 W_\mu^3 + g_a Y_a X_{a\mu} + g_b Y_b X_{b\mu}\,. \tag{5.26}$$

For that end, we will do as in Chapter 2 and explore the definition of electromagnetic charge in this context. In a general sense, it is a linear combination of the operators above

$$Q = cT_3 + aY_a + bY_b\,. \tag{5.27}$$

It will prove instructive to look first at the case where at least one of the multiplets of the theory is a singlet, and after that expand to the more general case.

5.2.1 Theories with a Singlet

As discussed in Chapter 2, for the electromagnetic charge to be conserved, when it is applied to the vacuum of each multiplet in the theory, it must give zero

$$Q < \phi_i >= (ct_{3Vi} + ay_{ai} + by_{bi}) < \phi_i >= 0\,. \tag{5.28}$$

The singlets in the theory have automatically $t_{3Vi} = 0$. The condition on their hypercharges is then

$$a y_{asi} + b y_{bsi} = 0 \,, \tag{5.29}$$

where I'm using the s subscript to indicate only the singlets. This implies that all singlet hypercharges must have the same ratio

$$\frac{y_{asi}}{y_{bsi}} = \frac{y_{asj}}{y_{bsj}} = -\frac{b}{a} \,. \tag{5.30}$$

One can then always apply a rotation of $X_{a\mu}$ and $X_{b\mu}$ to the basis with a gauge field B_μ that does not couple to any of the singlets, and a gauge field X_μ that couples to all the singlets. The previous expressions become then (see Equations (5.43)-(5.46) below)

$$K^0_\mu = \quad g T_3 W^3_\mu + g_B Y_B B_\mu + g_X Y_X X_\mu \,, \tag{5.31}$$

$$Q = \quad c T_3 + d Y_B + d' Y_X \,, \tag{5.32}$$

$$Q < \phi_i >= \quad (c t_{3Vi} + d y_{Bi} + d' y_{Xi}) < \phi_i >= 0 \,. \tag{5.33}$$

Applying to the singlets, this expression for the charge leads now to

$$d' y_{Xsi} = 0 \,. \tag{5.34}$$

And, since the singlets couple to the X_μ, we must have $d' = 0$.

In other words, and using the results in Appendix D, in an $SU(2) \times U(1) \times U(1)$ theory with at least one singlet, the photon must be orthogonal to the gauge boson X_μ that interacts with the singlets. Thus, one can define the angle θ_W rotating the W^3_μ and B_μ bosons to the photon as

$$\begin{pmatrix} Z^0_\mu \\ A_\mu \end{pmatrix} = \begin{pmatrix} \cos\theta_W & -\sin\theta_W \\ \sin\theta_W & \cos\theta_W \end{pmatrix} \begin{pmatrix} W^3_\mu \\ B_\mu \end{pmatrix} \,, \tag{5.35}$$

where Z^0_μ is not yet a physical particle. Then, one can define a second angle θ_X, mixing the resulting Z^0_μ with the remaining X_μ, to bring them to the physical basis as

$$\begin{pmatrix} Z'_\mu \\ Z_\mu \end{pmatrix} = \begin{pmatrix} \cos\theta_X & -\sin\theta_X \\ \sin\theta_X & \cos\theta_X \end{pmatrix} \begin{pmatrix} Z^0_\mu \\ X_\mu \end{pmatrix} \,. \tag{5.36}$$

The charge can once again be written as

$$Q = T_3 + r Y_B \,, \tag{5.37}$$

and, by applying it to the vacua, one can recover the formulas for θ_W and e of Section 2.3:

$$\cos(\theta_W) = \frac{rg}{\sqrt{r^2g^2 + g'^2}}\,, \tag{5.38}$$

$$\sin(\theta_W) = \frac{g'}{\sqrt{r^2g^2 + g'^2}}\,, \tag{5.39}$$

and

$$e = \frac{gg'}{\sqrt{g^2r^2 + g'^2}}\,. \tag{5.40}$$

For the rest one needs to use the results of Section 5.1 as we will show with an example at the end of this Chapter.

We conclude that, even though the theory has three neutral gauge bosons, there are only two physical angles needed to bring these fields to the physical basis, instead of the usual three Euler angles. This happens because one of them depends on the $U(1) \times U(1)$ basis in which we decide to start in, and is thus non physical. This third angle can be removed without loss of generality, by starting from the basis where the singlets couple exclusively to one gauge boson (X_μ). In the next section this will be proven to be true also for the case where there are no singlets in the theory.

5.2.2 Theories without a Singlet

It is assumed the existence of the photon that can be written as

$$A_\mu = cW^3_\mu + aX_{a\mu} + bX_{b\mu}\,, \tag{5.41}$$

and that, according to the results in D, corresponds to the unbroken charge

$$eQ = cgT^3 + ag_aY_a + bg_bY_b\,, \tag{5.42}$$

where $a^2 + b^2 + c^2 = 1$.

By rotating the $U(1) \times U(1)$ fields as

$$B_\mu = \frac{1}{\sqrt{a^2 + b^2}}(aX_{a\mu} + bX_{b\mu})\,, \tag{5.43}$$

$$X_\mu = \frac{1}{\sqrt{a^2 + b^2}}(bX_{a\mu} - aX_{b\mu})\,, \tag{5.44}$$

and the hypercharges as

$$g_BY_B = \frac{1}{\sqrt{a^2 + b^2}}(ag_aY_a + bg_bY_b)\,, \tag{5.45}$$

$$g_XY_X = \frac{1}{\sqrt{a^2 + b^2}}(bg_aY_a - ag_bY_b)\,, \tag{5.46}$$

K^0_μ gets rewritten as

$$K^0_\mu = gT_3W^3_\mu + g_BY_BB_\mu + g_XY_XX_\mu\,, \tag{5.47}$$

while the photon becomes

$$A_\mu = cW^3_\mu + dB_\mu\,, \tag{5.48}$$

where $d = \sqrt{a^2+b^2}$ so that $c^2+d^2=1$. In this basis, the electromagnetic charge is then

$$eQ = cgT^3 + dg_BY_B\,. \tag{5.49}$$

What we showed here is nothing more than proving that there is always a specific gauge boson lying within the $U(1)\times U(1)$ bosons space who is perpendicular to the photon. In the case of theories with singlets, this coincides with the one that does not couple to the singlets, but it is also existent in the other theories. This means that, regardless of our theory, if there is an unbroken $U(1)$, one can choose to start in a basis where there are only two angles needed to bring the gauge bosons to their physical basis, as described before, rendering the third Euler angle nonphysical.

5.3 Working Theory: Doublet plus Multiplet

As an example of the usage of the results obtained in this chapter so far, let us study the model with an $SU(2)_L \times U(1)_Y \times U(1)'$ Gauge symmetry, and a doublet and higher multiplet in the scalar sector, parameterized as

$$\varphi = \begin{pmatrix} . \\ \frac{1}{\sqrt{2}}(v+\varphi_R+i\varphi_I) \end{pmatrix} \quad , \quad \chi = \begin{pmatrix} . \\ . \\ \frac{1}{\sqrt{2}}(u+\chi_R+i\chi_I) \\ . \end{pmatrix}\,, \tag{5.50}$$

with hipercharges:

$$\varphi: \quad t_{3V} = -1/2 \quad y_B = 1/2 \quad y_X = y_2\,, \tag{5.51}$$

$$\chi: \quad t_{3V} = -y_B \quad y_B = y_B \quad y_X = y_X\,, \tag{5.52}$$

where we are already in the basis where X^μ is perpendicular to the photon, and implying that the constant in the electromagnetic charge of Equations (5.37) and (5.40) is $r=1$.

The C matrix may then be written as

$$C = \begin{pmatrix} -\frac{1}{2}gv & \frac{1}{2}g_Bv & y_2g_Xv \\ -y_Bgu & y_Bg_Bu & y_Xg_Xu \end{pmatrix}\,. \tag{5.53}$$

To turn this matrix square, we already know that there is only one massless boson in this theory, the photon, and find it using Equations (5.35), (5.38) and (5.39). And the C matrix rotates to

$$C' = \begin{pmatrix} -\frac{1}{2}g_0 v & 0 & y_2 g_X v \\ -y_B g_0 u & 0 & y_X g_X u \end{pmatrix} . \tag{5.54}$$

As discussed before, we can safely retrieve the photon from our calculations, loosing the null column of C' to get

$$C' = \begin{pmatrix} -\frac{1}{2}g_0 v & y_2 g_X v \\ -y_B g_0 u & y_X g_X u \end{pmatrix} . \tag{5.55}$$

The mass matrix will then be

$$M'^2 = \begin{pmatrix} g_0^2(\frac{1}{4}v^2 + y_B^2 u^2) & -g_0 g_x(\frac{1}{2}y_2 v^2 + y_B y_X u^2) \\ -g_0 g_x(\frac{1}{2}y_2 v^2 + y_B y_X u^2) & g_X^2(y_2^2 v^2 + y_X^2 u^2) \end{pmatrix} . \tag{5.56}$$

If we diagonalize this matrix we get to the physical basis. Lets then say that this matrix is diagonalized by the rotation matrix

$$R_X = \begin{pmatrix} \cos\theta_X & -\sin\theta_X \\ \sin\theta_X & \cos\theta_X \end{pmatrix} , \tag{5.57}$$

such that

$$R_X M'^2 R_X^T = M_D^2 , \tag{5.58}$$

or, equivalently:

$$C' R_X^T = C_D = \begin{pmatrix} \bar{v}_{D1} & \bar{v}_{D2} \end{pmatrix} \quad , \quad \bar{v}_{D1} \cdot \bar{v}_{D2} = 0 . \tag{5.59}$$

Assuming $\theta_X \in [-\pi/4, \pi/4]$, these give us expressions for θ_X

$$\cos\theta_X = \sqrt{\frac{1 + \sqrt{1 - 1/(1 + K^2/4)}}{2}} , \tag{5.60}$$

$$\sin\theta_X = \frac{sign(K)}{c_X\sqrt{4 + K^2}} , \tag{5.61}$$

where:

$$K = \frac{g_0^2(\frac{1}{4}v^2 + y_B^2 u^2) - g_X^2(y_2^2 v^2 + y_X^2 u^2)}{\frac{1}{2}g_0 g_X(\frac{1}{2}y_2 v^2 + y_B y_X u^2)} . \tag{5.62}$$

The coupling matrix in the physical basis becomes:

$$C_D = -\begin{pmatrix} v(\frac{1}{2}g_0 c_X + y_2 g_X s_X) & v(\frac{1}{2}g_0 s_X - y_2 g_X c_X) \\ u(y_B g_0 c_X + y_X g_X s_X) & u(y_B g_0 s_X - y_X g_X c_X) \end{pmatrix}, \tag{5.63}$$

and the masses of the Gauge bosons are:

$$M_1^2 = v^2(\frac{1}{2}g_0 c_X + y_2 g_X s_X)^2 + u^2(y_B g_0 c_X + y_X g_X s_X)^2\,, \tag{5.64}$$

$$M_2^2 = v^2(\frac{1}{2}g_0 s_X - y_2 g_X c_X)^2 + u^2(y_B g_0 s_X - y_X g_X c_X)^2\,. \tag{5.65}$$

The Goldstone bosons absorbed by each Gauge boson are:

$$G_1 = \frac{v(\frac{1}{2}g_0 c_X + y_2 g_X s_X)\varphi_I + u(y_B g_0 c_X + y_X g_X s_X)\chi_I}{M_1}\,, \tag{5.66}$$

$$G_2 = \frac{v(\frac{1}{2}g_0 s_X - y_2 g_X c_X)\varphi_I + u(y_B g_0 s_X - y_X g_X c_X)\chi_I}{M_2}\,, \tag{5.67}$$

with coupling constants $-M_1$ and $-M_2$ with their respective Gauge boson.

Chapter 6

Conclusions

We started by introducing topics in Multi-Higgs physics to introduce the notation used in the text and to give the reader a different approach on those topics. A discussion on custodial symmetry leads us to study models with that property.

The study of models with an arbitrary number of doublets and singlets lead us to identify the presence of an understudied coupling between the Z boson and two charged scalars of different mass. We justify why this coupling is only present in theories with at least two doublets and a charged singlet. We call the minimal models containing such a sector Zee-type models.

As an example of a Zee-type model, used to search for signals of this kind of couplings, we use a Zee model composed of a type 2 2HDM plus a charged scalar singlet. We study the scalar sector of this model including the rotation to the physical basis and the inversion of the parameters of the potential into physical quantities.

We study and impose various theoretical constraint on the model. For the study of the bounded from below conditions, we use the study made in Reference [25]. One of the condition on α and β cannot be solved analytically, so we took a large sample of those parameters and excluded the ones not satisfying the condition. For the charged breaking minima analysis, we took an approach based on Reference [25]. Perturbative unitarity of the quartic couplings was ensured by the implementation of the general algorithm presented in Reference [26]. We use the fit given in Reference [27] to the electroweak precision measurements and demand the parameters to be within 2σ of the result.

We also imposed experimental constraints on the model. The constraints on the measured Higgs boson of $125GeV$ were taken from Reference [29]. The constraints on other neutral and charged scalars were implemented using the most recent version of `HiggBounds 5` [30].

The last constraints we made on the model are from the $B \to X_s\gamma$ decay. We started by studding this constraints on the simpler type 2 2HDM, using a calculation close to the original in Reference [17], and reproducing the result in Reference [18] of a lower bound of $580GeV$ on the charged scalar. We then imposed the constraints on our type 2 Zee model, and found that, in this model, only one of the charged scalars needs to satisfy the $580GeV$ lower bound, while the other can be as low as $50GeV$. We also checked that when γ, the rotation angle of the charged scalars, equals zero, we recover the type 2

2HDM result as expected, while for γ closer to $\pm\pi/2$ we get the less restrained parameter space.

The first process where we looked for an impact of the coupling of interest, was the decay of the measured higgs boson into $Z\gamma$. The decay into $\gamma\gamma$ has the same diagrams as in theories with two charged scalars but without this coupling, as in the 3HDM. But the decay into $Z\gamma$ has those diagrams plus diagrams with different charged scalars running in the same loop, exclusive to this models. We calculated all those diagrams and found the expected dependence on γ and, consequently on our coupling of interest. Nonetheless, once we summed all the diagrams, this dependence was completely lost. Meaning that the overall process has no new properties when compared to models like the 3HDM, which do not present this type of coupling.

We then turned to a more obvious way of probing such a coupling, the decay $H_2^+ \to H_1^+ + Z$, unique to this type of models. We verified that this decay does happen for a mass of the heaviest charged scalar above the $580GeV$ limit, as expected from the $B \to X_s\gamma$ analysis, and that it has the predicted strong dependence on our coupling of interest, or, equivalently, on the angle γ. We explain that the chain of events composed of this decay followed by the decay of the resulting scalar into a top bottom pair should have very clear signatures at colliders. We strongly urge a search for these kind of signatures.

To test the relevance of this process, we generate benchmark points in relevant benchmark regions. We successfully generated three benchmark regions where the decays of our process are the most prominent. There is still a need for background studies to be done, but these should, in principle, provide clear signatures. The first of these benchmark regions has the masses of both charged scalars above the $580GeV$ limit, while the other two have the mass of the lighter one considerably below that limit, proving that there are indeed good points where one of the scalars does not satisfy that lower bound.

We also took a forth benchmark region with different characteristics. The decay $H_1^+ \to W^+ + h_1$ is one of the channels that have not been investigated at the LHC yet [44]. This last benchmark region was taken from the few points with a large BR($H_1^+ \to W^+ + h_1$). We find that both BR($H_1^+ \to W^+ + h_1$) and BR($H_1^+ \to W^+ + h_2$) can be sizeable, but in this case, the BR($H_2^+ \to H_1^+ + Z$) is very small. Nonetheless, BR($H_2^+ \to W^+ + h_1$) and BR($H_2^+ \to W^+ + h_2$) can also be large, which makes this an interesting benchmark region.

Finally, we study models with extended gauge symmetries in the electroweak sector. We start by explicitly applying the Higgs mechanism to the neutral gauge bosons of such theories. Then we study how the addiction of an $U(1)$ symmetry affects the definition of charge and the rotation of the gauge bosons into the physical basis. We conclude that, despite of having three gauge bosons, only two angles are needed to bring them to the mass eigenstates, since the third is rendered nonphysical by the freedom in deciding in which $U(1) \times U(1)$ basis we start in. We end by applying the previous concepts to an $SU(2) \times U(1) \times U(1)$ theory with a doublet and a higher multiplet. We deduce formulas for this model that might be useful in future work.

Bibliography

[1] S. Glashow, *Partial Symmetries of Weak Interactions*, *Nucl.Phys.* **22** (1961) 579–588.

[2] S. Weinberg, *A model of leptons*, *Phys. Rev. Lett.* **19** (1967) 1264–1266.

[3] A. Salam, *Weak and electromagnetic interactions*, *Conf.Proc.* **C680519** (1968) 367–377. Originally printed in Svartholm: Elementary Particle Theory, Proceedings of the Nobel Symposium held 1968 at Lerum, Sweden, Stockholm.

[4] **ATLAS** Collaboration, G. Aad *et. al.*, *Observation of a new particle in the search for the Standard Model Higgs boson with the ATLAS detector at the LHC*, *Phys. Lett. B* **716** (2012) 1–29, [1207.7214].

[5] **CMS** Collaboration, S. Chatrchyan *et. al.*, *Observation of a New Boson at a Mass of 125 GeV with the CMS Experiment at the LHC*, *Phys. Lett. B* **716** (2012) 30–61, [1207.7235].

[6] P. W. Higgs, *Broken symmetries, massless particles and gauge fields*, *Phys. Lett.* **12** (1964) 132–133.

[7] F. Englert and R. Brout, *Broken Symmetry and the Mass of Gauge Vector Mesons*, *Phys.Rev.Lett.* **13** (1964) 321–322.

[8] A. Zee, *A theory of lepton number violation, neutrino majorana mass, and oscillation*, *Phys. Lett.* **B93** (1980) 389.

[9] A. Y. Smirnov and M. Tanimoto, *Is Zee model the model of neutrino masses?*, Phys. Rev. D **55** (1997), 1665-1671 doi:10.1103/PhysRevD.55.1665 [arXiv:hep-ph/9604370 [hep-ph]].

[10] L. M. Krauss, S. Nasri and M. Trodden, *A Model for neutrino masses and dark matter*, Phys. Rev. D **67** (2003), 085002 doi:10.1103/PhysRevD.67.085002 [arXiv:hep-ph/0210389 [hep-ph]].

[11] L. Wolfenstein, *A Theoretical Pattern for Neutrino Oscillations*, Nucl. Phys. B **175** (1980), 93-96 doi:10.1016/0550-3213(80)90004-8

[12] Y. Koide, *Can the Zee model explain the observed neutrino data?*, Phys. Rev. D **64** (2001), 077301 doi:10.1103/PhysRevD.64.077301 [arXiv:hep-ph/0104226 [hep-ph]].

[13] X. G. He, *Is the Zee model neutrino mass matrix ruled out?*, Eur. Phys. J. C **34** (2004), 371-376 doi:10.1140/epjc/s2004-01669-8 [arXiv:hep-ph/0307172 [hep-ph]].

[14] J. Herrero-García, T. Ohlsson, S. Riad and J. Wirén, *Full parameter scan of the Zee model: exploring Higgs lepton flavor violation*, JHEP **04** (2017), 130 doi:10.1007/JHEP04(2017)130 [arXiv:1701.05345 [hep-ph]].

[15] K. S. Babu, P. S. B. Dev, S. Jana and A. Thapa, *Non-Standard Interactions in Radiative Neutrino Mass Models*, JHEP **03** (2020), 006 doi:10.1007/JHEP03(2020)006 [arXiv:1907.09498 [hep-ph]].

[16] Ricardo R. Florentino and Jorge C. Romão and João P. Silva, *Off diagonal charged scalar couplings with the Z boson: the Zee model as an example*, 2106.08332.

[17] F. Borzumati and C. Greub, *2HDMs predictions for anti-B —> X(s) gamma in NLO QCD*, *Phys. Rev. D* **58** (1998) 074004, [hep-ph/9802391].

[18] M. Misiak and M. Steinhauser, *Weak radiative decays of the B meson and bounds on $M_{H^\pm}$ in the Two-Higgs-Doublet Model*, *Eur. Phys. J. C* **77** (2017), no. 3 201, [1702.04571].

[19] W. Grimus, L. Lavoura, O. M. Ogreid, and P. Osland, *A Precision constraint on multi-Higgs-doublet models*, *J. Phys.* **G35** (2008) 075001, [0711.4022].

[20] M. P. Bento, H. E. Haber, J. C. Romão, and J. P. Silva, *Multi-Higgs doublet models: the Higgs-fermion couplings and their sum rules*, *JHEP* **10** (2018) 143, [1808.07123].

[21] G. C. Branco, P. M. Ferreira, L. Lavoura, M. N. Rebelo, M. Sher, and J. P. Silva, *Theory and phenomenology of two-Higgs-doublet models*, *Phys. Rept.* **516** (2012) 1–102, [1106.0034].

[22] F. Botella and J. P. Silva, *Jarlskog - like invariants for theories with scalars and fermions*, *Phys. Rev. D* **51** (1995) 3870–3875, [hep-ph/9411288].

[23] S. Kanemura, T. Kubota, and E. Takasugi, *Lee-Quigg-Thacker bounds for Higgs boson masses in a two doublet model*, *Phys. Lett. B* **313** (1993) 155–160, [hep-ph/9303263].

[24] P. M. Ferreira, R. Santos, and A. Barroso, *Stability of the tree-level vacuum in two Higgs doublet models against charge or CP spontaneous violation*, *Phys. Lett. B* **603** (2004) 219–229, [hep-ph/0406231]. [Erratum: Phys.Lett.B 629, 114–114 (2005)].

[25] A. Barroso and P. M. Ferreira, *Charge breaking bounds in the Zee model*, *Phys. Rev. D* **72** (2005) 075010, [hep-ph/0507128].

[26] M. P. Bento, H. E. Haber, J. C. Romão, and J. P. Silva, *Multi-Higgs doublet models: physical parametrization, sum rules and unitarity bounds*, 1708.09408.

[27] **Gfitter Group** Collaboration, M. Baak, J. Cúth, J. Haller, A. Hoecker, R. Kogler, K. Mönig, M. Schott, and J. Stelzer, *The global electroweak fit at NNLO and prospects for the LHC and ILC*, *Eur. Phys. J. C* **74** (2014) 3046, [1407.3792].

[28] W. Grimus, L. Lavoura, O. Ogreid, and P. Osland, *The Oblique parameters in multi-Higgs-doublet models*, *Nucl. Phys. B* **801** (2008) 81–96, [0802.4353].

[29] **ATLAS** Collaboration, G. Aad *et. al.*, *Combined measurements of Higgs boson production and decay using up to* $80\ fb^{-1}$ *of proton-proton collision data at* $\sqrt{s} = 13$ *TeV collected with the ATLAS experiment*, *Phys. Rev. D* **101** (2020), no. 1 012002, [1909.02845].

[30] P. Bechtle, D. Dercks, S. Heinemeyer, T. Klingl, T. Stefaniak, G. Weiglein, and J. Wittbrodt, *HiggsBounds-5: Testing Higgs Sectors in the LHC 13 TeV Era*, *Eur. Phys. J. C* **80** (2020), no. 12 1211, [2006.06007].

[31] F. Borzumati and C. Greub, *Two Higgs doublet model predictions for anti-B —> X(s) gamma in NLO QCD: Addendum*, *Phys. Rev. D* **59** (1999) 057501, [hep-ph/9809438].

[32] M. Misiak, *Radiative Decays of the* B *Meson: a Progress Report*, *Acta Phys. Polon. B* **49** (2018) 1291–1300.

[33] A. G. Akeroyd, S. Moretti, T. Shindou, and M. Song, *CP asymmetries of* $\overline{B} \to X_s/X_d\gamma$ *in models with three Higgs doublets*, *Phys. Rev. D* **103** (2021), no. 1 015035, [2009.05779].

[34] **SIMBA** Collaboration, F. U. Bernlochner, H. Lacker, Z. Ligeti, I. W. Stewart, F. J. Tackmann, and K. Tackmann, *Precision Global Determination of the* $B \to X_s\gamma$ *Decay Rate*, 2007.04320.

[35] M. Misiak, A. Rehman, and M. Steinhauser, *Towards* $\overline{B} \to X_s\gamma$ *at the NNLO in QCD without interpolation in* m_c, *JHEP* **06** (2020) 175, [2002.01548].

[36] **HFLAV** Collaboration, Y. S. Amhis *et. al.*, *Averages of* b*-hadron,* c*-hadron, and* τ*-lepton properties as of 2018*, 1909.12524.

[37] **Particle Data Group** Collaboration, P. A. Zyla *et. al.*, *Review of Particle Physics*, *PTEP* **2020** (2020), no. 8 083C01.

[38] M. Chakraborti, D. Das, M. Levy, S. Mukherjee, and I. Saha, *Prospects of light charged scalars in a three Higgs doublet model with* Z_3 *symmetry*, 2104.08146.

[39] P. M. Ferreira, J. F. Gunion, H. E. Haber and R. Santos, *Probing wrong-sign Yukawa couplings at the LHC and a future linear collider*, Phys. Rev. D **89** (2014) no.11, 115003 doi:10.1103/PhysRevD.89.115003 [arXiv:1403.4736 [hep-ph]].

[40] D. Fontes, J. C. Romão and J. P. Silva, *A reappraisal of the wrong-sign* $hb\bar{b}$ *coupling and the study of* $h \to Z\gamma$, Phys. Rev. D **90** (2014) no.1, 015021 doi:10.1103/PhysRevD.90.015021 [arXiv:1406.6080 [hep-ph]].

[41] D. Fontes, J. C. Romão, and J. P. Silva, $h \to Z\gamma$ *in the complex two Higgs doublet model*, *JHEP* **12** (2014) 043, [1408.2534].

[42] R. Boto, J. C. Romão, and J. P. Silva, *to appear*.

[43] A. Djouadi, *The Anatomy of electro-weak symmetry breaking. I: The Higgs boson in the standard model*, *Phys. Rept.* **457** (2008) 1–216, [hep-ph/0503172].

[44] H. Bahl, T. Stefaniak, and J. Wittbrodt, *The forgotten channels: charged Higgs boson decays to a $W^{\pm}$ and a non-SM-like Higgs boson*, 2103.07484.

[45] C. Degrande, K. Hartling, H. E. Logan, A. D. Peterson, and M. Zaro, *Automatic predictions in the Georgi-Machacek model at next-to-leading order accuracy*, *Phys. Rev. D* **93** (2016), no. 3 035004, [1512.01243].

[46] C. Degrande, R. Frederix, V. Hirschi, M. Ubiali, M. Wiesemann, and M. Zaro, *Accurate predictions for charged Higgs production: Closing the $m_{H^{\pm}} \sim m_t$ window*, *Phys. Lett. B* **772** (2017) 87–92, [1607.05291].

[47] **ATLAS** Collaboration, *Search for charged Higgs bosons decaying into a top-quark and a bottom-quark at $\sqrt{s}$ = 13 TeV with the ATLAS detector*, .

Appendix A

Couplings of the charged Higgs

A.1 Couplings to the Z boson

We define the coupling as

$$[H_j^+, H_k^-, Z] := -i\,\frac{g}{2c_W}(p_{H_j^+} - p_{H_k^-})^\mu g_{\mathrm{HpjHmkZ}}[j,k], \tag{A.1}$$

where all particles are entering the vertex and

$$g_{\mathrm{HpjHmkZ}}[1,1] = \frac{1}{2}\left(c_W^2 - 3s_W^2 + \cos(2\gamma)\right), \tag{A.2a}$$

$$g_{\mathrm{HpjHmkZ}}[1,2] = -\frac{1}{2}\sin(2\gamma), \tag{A.2b}$$

$$g_{\mathrm{HpjHmkZ}}[2,1] = -\frac{1}{2}\sin(2\gamma), \tag{A.2c}$$

$$g_{\mathrm{HpjHmkZ}}[2,2] = \frac{1}{2}\left(c_W^2 - 3s_W^2 - \cos(2\gamma)\right), \tag{A.2d}$$

Notice that when the mixing angle γ vanishes the singlet decouples from the doublet and there is no $[H_j^+, H_k^-, Z]$ vertex for $j \neq k$.

A.2 Couplings to the W boson

For CP even neutral Higgs bosons ($j = 1, 2$) we define the coupling as

$$[h_j, H_k^+, W^-] : -i\,\frac{g}{2}(p_{H_k^+} - p_{h_j})^\mu g_{\mathrm{hjHpkWm}}[j,k], \tag{A.3}$$

where all particles are entering the vertex. For CP odd neutral Higgs boson ($j = 3$) we define

$$[h_3, H_k^+, W^-] := \frac{g}{2}(p_{h_3} - p_{H_k^+})^\mu g_{\mathrm{hjHpkWm}}[3,k], \tag{A.4}$$

where

$$g_{\mathrm{hjHpkWM}}[1,1] = \cos(\gamma)\sin(\alpha-\beta)), \tag{A.5a}$$

$$g_{\mathrm{hjHpkWM}}[1,2] = -\sin(\alpha-\beta)\sin(\gamma), \tag{A.5b}$$

$$g_{\mathrm{hjHpkWM}}[2,1] = \cos(\alpha-\beta)\cos(\gamma), \tag{A.5c}$$

$$g_{\mathrm{hjHpkWM}}[2,2] = -\cos(\alpha-\beta)\sin(\gamma), \tag{A.5d}$$

$$g_{\mathrm{hjHpkWM}}[3,1] = \cos(\gamma), \tag{A.5e}$$

$$g_{\mathrm{hjHpkWM}}[3,2] = -\sin(\gamma), \tag{A.5f}$$

A.3 Couplings to quarks and leptons

The interactions of charged Higgs bosons with quarks are given by the following Lagrangian

$$\mathcal{L} = \frac{g}{\sqrt{2}}\left[\frac{m_{d_j}}{M_W}X_k\overline{u}_i V_{ij} P_R d_j + \frac{m_{u_i}}{M_W}X_k\overline{u}_i V_{ij} Y_k P_L d_j + \frac{m_l}{M_W}Z_k\overline{\nu}_l P_R e_l\right] H_k^+ + \text{h.c.} \tag{A.6}$$

where $k = 1, 2$ and we have used the conventions of Borzumati and Greub [17], extended in Reference [33], which is convenient for the BR($B \to X_s\gamma$) calculation. We get

$$X_1 = \tan\beta\cos\gamma, \qquad Y_1 = \cot\beta\cos\gamma, \qquad Z_1 = \tan\beta\cos\gamma, \tag{A.7a}$$

$$X_2 = -\tan\beta\sin\gamma, \qquad Y_2 = -\cot\beta\sin\gamma, \qquad Z_2 = -\tan\beta\sin\gamma, \tag{A.7b}$$

A.4 Couplings to neutral Higgs

Finally the couplings to the neutral Higgs are given by the Lagrangian

$$\mathcal{L} = H_i^+ H_k^- h_j g_{\mathrm{hjHpiHmk}}[j,i,k], \tag{A.8}$$

where g_{hjHpiHmk} are long expressions that we do not reproduce here. Note however that $g_{\mathrm{hjHpiHmk}}(3,i,k) = 0$.

Appendix B

The decays $h \to \gamma\gamma$ and $h \to Z\gamma$

These decays were calculated for the 2HDM to one loop approximation in [41]. Since most terms in the Lagrangian of our model only differ by multiplicative constants, our results will only change by some factors. We adapt from [41] for the next results. The major difference occurs in $h \to Z\gamma$, where the presence of the $ZH_1^{\pm}H_2^{\mp}$ coupling allows for the new diagrams in Figure 4.5.

B.1 Fermion Loops

The fermion loops are easily obtained plugging the couplings of Equation (3.20) in the results of [41]:

$$
\begin{aligned}
X_F^{\gamma\gamma} &= -\sum_f N_c^f 2a_f^2 Q_f^2 \tau_f [1 + (1-\tau_f) f(\tau_f)] \,, \\
Y_F^{\gamma\gamma} &= -\sum_f N_c^f 2b_f^2 Q_f^2 \tau_f f(\tau_f) \,, \\
X_F^{Z\gamma} &= -\sum_f N_c^f \frac{4a_f^2 g_V^f Q_f m_f^2}{s_W c_W} \left[\frac{2M_Z^2}{(m_h^2 - M_Z^2)^2} \left[B_0(m_h^2, m_f^2, m_f^2) - B_0(M_Z^2, m_f^2, m_f^2) \right] \right. \\
&\quad \left. + \frac{1}{m_h^2 - M_Z^2} \left[(4m_f^2 - m_h^2 + M_Z^2) C_0(M_Z^2, 0, m_h^2, m_f^2, m_f^2, m_f^2) + 2 \right] \right] \,, \\
Y_F^{Z\gamma} &= -\sum_f N_c^f \frac{4b_f^2 g_V^f Q_f m_f^2}{s_W c_W} C_0(M_Z^2, 0, m_h^2, m_f^2, m_f^2, m_f^2) \,,
\end{aligned}
\tag{B.1}
$$

where N_c^f is 3 for quarks and 1 for leptons, Q_f is the fermion charge, g_V^f is the fermion's vector coupling to the Z boson and the sums run over all fermions f. The function appearing is defined as

$$
f(\tau) = -\frac{2m_f^2}{\tau_f} C_0(0, 0, m_h^2, m_f^2, m_f^2, m_f^2) = \begin{cases} \left[\sin^{-1}\left(\sqrt{1/\tau} \right) \right]^2 , & \text{if } \tau \geq 1 \\ -\frac{1}{4} \left[\ln\left(\frac{1+\sqrt{1-\tau}}{1-\sqrt{1-\tau}} \right) - i\pi \right]^2 , & \text{if } \tau < 1 \end{cases} \,, \tag{B.2}
$$

while B_0 and C_0 are the Passarino-Veltman functions.

B.2 Charged gauge boson loops

The only change in these loops comes from the hVV vertex, which is multiplied by a factor $\mathrm{Re}(\omega^\dagger V)^\beta$, and so is the loop. Using the notation of [41], we have

$$\begin{aligned} X_W^{\gamma\gamma} &= \mathrm{Re}(\omega^\dagger V)^\beta \left[2 + 3\tau_W + 3\tau_W(2-\tau_W) f(\tau_W)\right] , \\ X_W^{Z\gamma} &= \frac{\mathrm{Re}(\omega^\dagger V)^\beta}{\tan\theta_W} I_W , \end{aligned} \tag{B.3}$$

where,

$$\begin{aligned} \omega_a &= v_a/v, \quad \tau_W = \frac{4M_W^2}{m_h^2} , \\ I_W &= \frac{1}{(m_h^2 - M_Z^2)^2}\left[m_h^2(1-\tan^2\theta_W) - 2M_W^2(-5+\tan^2\theta_W)\right] M_Z^2 \Delta B_0 , \\ &\quad + \frac{1}{m_h^2 - M_Z^2}[m_h^2(1-\tan^2\theta_W) - 2M_W^2(-5+\tan^2\theta_W) , \\ &\quad + 2M_W^2\left[(-5+\tan^2\theta_W)(m_h^2 - 2M_W^2) - 2M_Z^2(-3+\tan^2\theta_W)\right] C_0\right] M_Z^2 \Delta B_0 , \\ \Delta B_0 &= B_0(m_h^2, M_W^2, M_W^2) - B_0(M_Z^2, M_W^2, M_W^2) , \\ C_0 &= C_0(M_Z^2, 0, m_h^2, M_W^2, M_W^2, M_W^2) . \end{aligned} \tag{B.4}$$

B.3 Charged Scalar Loops

For the decay to $\gamma\gamma$, the loops are the same as the one presented in [41] with the cubic scalar vertex replaced by the ones we defined in Equation (3.13). Besides this replacement, we only need to sum over the charged scalars, obtaining

$$X_H^{\gamma\gamma} = -\sum_\alpha \frac{g^{2\alpha\alpha}\, v^2}{2m_{\pm\alpha}^2} \tau_{\pm\alpha}[1 - \tau_{\pm\alpha} f(\tau_{\pm\alpha})] , \tag{B.5}$$

where $\tau_{\pm\alpha} = 4m_h^2/m_{\pm\alpha}$. Regarding the decay to $Z\gamma$, we can allow two different scalars to run within the same loop, as seen in Figure 4.5. This generalizes the result in [41]. We obtain

$$\begin{aligned} X_H^{Z\gamma} = -\sum_{\alpha_1\alpha_2} \frac{(2s_W^2\delta^{\alpha_1\alpha_2} - (U^\dagger U)^{\alpha_2\alpha_1})}{\sin\theta_W\cos\theta_W} \frac{g^{2\alpha_1\alpha_2}\, v^2}{m_h^2 - M_Z^2} \Bigg[\frac{M_Z^2}{m_h^2 - M_Z^2} \left(B_0(m_h^2, m_{\pm\alpha_1}^2, m_{\pm\alpha_2}^2)\right. \\ \left. - B_0(M_Z^2, m_{\pm\alpha_1}^2, m_{\pm\alpha_2}^2)\right) + 1 + m_{\pm\alpha_1}^2 C_0(M_Z^2, 0, m_h^2, m_{\pm\alpha_1}^2, m_{\pm\alpha_1}^2, m_{\pm\alpha_2}^2) \\ + m_{\pm\alpha_2}^2 C_0(M_Z^2, 0, m_h^2, m_{\pm\alpha_2}^2, m_{\pm\alpha_2}^2, m_{\pm\alpha_1}^2) \Bigg] . \end{aligned} \tag{B.6}$$

If there were no cubic terms in Equation (3.11) ($\mu_4^{abi} = 0$), then $(U^\dagger U)^{\alpha_2\alpha_1} = \delta^{\alpha_2\alpha_1}$ and there would be no diagrams involving simultaneously two different charged scalars.

B.4 Final widths for loop decays

The final widths are given by

$$\Gamma(h \to \gamma\gamma) = \frac{G_F \alpha^2 m_h^2}{128\sqrt{2}\pi^3} \left(|X_F^{\gamma\gamma} + X_W^{\gamma\gamma} + X_H^{\gamma\gamma}|^2 + |Y_F^{\gamma\gamma}|^2 \right) ,$$
$$\Gamma(h \to Z\gamma) = \frac{G_F \alpha^2 m_h^2}{64\sqrt{2}\pi^3} \left(1 - \frac{M_Z^2}{m_h^2} \right)^3 \left(|X_F^{Z\gamma} + X_W^{Z\gamma} + X_H^{Z\gamma}|^2 + |Y_F^{Z\gamma}|^2 \right) . \tag{B.7}$$

Appendix C

Perturbative unitarity

We write here the scattering matrices for the various (Q, Y) combinations and list all the eigenvalues at the end. This is presented here for the first time. We follow the notation of [26].

C.1 $Q = 2, Y = 1$

For the combination of states S_α^{++} in Equation (4.15a) we have

$$M_2^{++} = \begin{bmatrix} \lambda_1 & 0 & 0 & \lambda_5 & 0 & 0 \\ 0 & \lambda_3 + \lambda_4 & 0 & 0 & 0 & 0 \\ 0 & 0 & k_1 & 0 & -k_{12} & 0 \\ \lambda_5 & 0 & 0 & \lambda_2 & 0 & 0 \\ 0 & 0 & -k_{12} & 0 & k_2 & 0 \\ 0 & 0 & 0 & 0 & 0 & 2\lambda_c \end{bmatrix}. \tag{C.1}$$

C.2 $Q = 1, Y = 1$

For the combination of states S_α^{+} in Equation (4.15b) we have

$$M_2^{+} = \begin{bmatrix} \lambda_1 & 0 & 0 & \lambda_5 & 0 & 0 \\ 0 & \lambda_3 & \lambda_4 & 0 & 0 & 0 \\ 0 & \lambda_4 & \lambda_3 & 0 & 0 & 0 \\ \lambda_5 & 0 & 0 & \lambda_2 & 0 & 0 \\ 0 & 0 & 0 & 0 & k_1 & -k_{12} \\ 0 & 0 & 0 & 0 & -k_{12} & k_2 \end{bmatrix}. \tag{C.2}$$

C.3 $Q = 1, Y = 0$

For the combination of states T^+_α in Equation (4.15c) we have

$$M^+_0 = \begin{bmatrix} \lambda_1 & 0 & 0 & \lambda_4 & 0 & 0 \\ 0 & \lambda_3 & \lambda_5 & 0 & 0 & 0 \\ 0 & \lambda_5 & \lambda_3 & 0 & 0 & 0 \\ \lambda_4 & 0 & 0 & \lambda_2 & 0 & 0 \\ 0 & 0 & 0 & 0 & k_1 & -k_{12} \\ 0 & 0 & 0 & 0 & -k_{12} & k_2 \end{bmatrix} . \tag{C.3}$$

C.4 $Q = 0, Y = 1$

For the combination of states S^0_α in Equation (4.15d) we have

$$M^0_2 = \begin{bmatrix} 0 & 0 & 0 \\ 0 & 0 & 0 \\ 0 & 0 & 0 \end{bmatrix} . \tag{C.4}$$

C.5 $Q = 0, Y = 0$

For the combination of states T^0_α in Equation (4.15e) we have

$$M^0_0 = \begin{bmatrix} 2\lambda_1 & 0 & 0 & 0 & \lambda_{34} & 0 & 0 & 0 & k_1 & \lambda_1 & 0 & 0 & \lambda_3 \\ 0 & 2\lambda_5 & 0 & \lambda_{34} & 0 & 0 & 0 & 0 & -k_{12} & 0 & \lambda_5 & \lambda_4 & 0 \\ 0 & 0 & 0 & 0 & 0 & 0 & k_1 & -k_{12} & 0 & 0 & 0 & 0 & 0 \\ 0 & \lambda_{34} & 0 & 2\lambda_5 & 0 & 0 & 0 & 0 & -k_{12} & 0 & \lambda_4 & \lambda_5 & 0 \\ \lambda_{34} & 0 & 0 & 0 & 2\lambda_2 & 0 & 0 & 0 & k_2 & \lambda_3 & 0 & 0 & \lambda_2 \\ 0 & 0 & 0 & 0 & 0 & 0 & -k_{12} & k_2 & 0 & 0 & 0 & 0 & 0 \\ 0 & 0 & k_1 & 0 & 0 & -k_{12} & 0 & 0 & 0 & 0 & 0 & 0 & 0 \\ 0 & 0 & -k_{12} & 0 & 0 & k_2 & 0 & 0 & 0 & 0 & 0 & 0 & 0 \\ k_1 & -k_{12} & 0 & -k_{12} & k_2 & 0 & 0 & 0 & 4\lambda_c & k_1 & -k_{12} & -k_{12} & k_2 \\ \lambda_1 & 0 & 0 & 0 & \lambda_3 & 0 & 0 & 0 & k_1 & 2\lambda_1 & 0 & 0 & \lambda_{34} \\ 0 & \lambda_5 & 0 & \lambda_4 & 0 & 0 & 0 & 0 & -k_{12} & 0 & 2\lambda_5 & \lambda_{34} & 0 \\ 0 & \lambda_4 & 0 & \lambda_5 & 0 & 0 & 0 & 0 & -k_{12} & 0 & \lambda_{34} & 2\lambda_5 & 0 \\ \lambda_3 & 0 & 0 & 0 & \lambda_2 & 0 & 0 & 0 & k_2 & \lambda_{34} & 0 & 0 & 2\lambda_2 \end{bmatrix} , \tag{C.5}$$

where for simplicity we have defined

$$\lambda_{34} \equiv \lambda_3 + \lambda_4 . \tag{C.6}$$

C.6 The independent eigenvalues

We can obtain easily the eigenvalues for all the matrices except for M_0^0 in Equation (C.5) for which we have to solve numerically a fourth order polynomial. The list of independent eigenvalues is,

$$\Lambda_1 = \frac{1}{2}\left(-\sqrt{(k_1)^2 - 2k_1k_2 + 4(k_{12})^2 + (k_2)^2} + k_1 + k_2\right), \tag{C.7a}$$

$$\Lambda_2 = \frac{1}{2}\left(\sqrt{(k_1)^2 - 2k_1k_2 + 4(k_{12})^2 + (k_2)^2} + k_1 + k_2\right), \tag{C.7b}$$

$$\Lambda_3 = \lambda_3 + \lambda_4 \tag{C.7c}$$

$$\Lambda_4 = \frac{1}{2}\left(-\sqrt{\lambda_1^2 - 2\lambda_1\lambda_2 + \lambda_2^2 + 4\lambda_5^2} + \lambda_1 + \lambda_2\right), \tag{C.7d}$$

$$\Lambda_5 = \frac{1}{2}\left(\sqrt{\lambda_1^2 - 2\lambda_1\lambda_2 + \lambda_2^2 + 4\lambda_5^2} + \lambda_1 + \lambda_2\right), \tag{C.7e}$$

$$\Lambda_6 = 2\lambda_c\,, \tag{C.7f}$$

$$\Lambda_7 = \lambda_3 - \lambda_4\,, \tag{C.7g}$$

$$\Lambda_8 = \frac{1}{2}\left(-\sqrt{\lambda_1^2 - 2\lambda_1\lambda_2 + \lambda_2^2 + 4\lambda_4^2} + \lambda_1 + \lambda_2\right), \tag{C.7h}$$

$$\Lambda_9 = \frac{1}{2}\left(\sqrt{\lambda_1^2 - 2\lambda_1\lambda_2 + \lambda_2^2 + 4\lambda_4^2} + \lambda_1 + \lambda_2\right), \tag{C.7i}$$

$$\Lambda_{10} = \lambda_3 - \lambda_5\,, \tag{C.7j}$$

$$\Lambda_{11} = \lambda_3 + \lambda_5\,, \tag{C.7k}$$

$$\Lambda_{12} = \frac{1}{2}\left(-\sqrt{(k_1)^2 - 2k_1k_2 + 4(k_{12})^2 + (k_2)^2} - k_1 - k_2\right), \tag{C.7l}$$

$$\Lambda_{13} = \frac{1}{2}\left(\sqrt{(k_1)^2 - 2k_1k_2 + 4(k_{12})^2 + (k_2)^2} - k_1 - k_2\right), \tag{C.7m}$$

$$\Lambda_{14} = \lambda_5 - \lambda_3\,, \tag{C.7n}$$

$$\Lambda_{15} = -\lambda_3 - 2\lambda_4 + 3\lambda_5\,. \tag{C.7o}$$

The remaining eigenvalues, $\Lambda_{16} - \Lambda_{19}$, are the roots of the polynomial of fourth degree

$$c_0 + c_1\,\eta + c_2\,\eta^2 + c_3\,\eta^2 + c_4\,\eta^4 = 0\,, \tag{C.8}$$

where

$$
\begin{aligned}
c_0 =& 6(k_1)^2\lambda_2\lambda_3 + 12(k_1)^2\lambda_2\lambda_4 + 18(k_1)^2\lambda_2\lambda_5 - 8k_1k_2\lambda_3^2 - 20k_1k_2\lambda_3\lambda_4 \\
&- 24k_1k_2\lambda_3\lambda_5 - 8k_1k_2\lambda_4^2 - 12k_1k_2\lambda_4\lambda_5 + 36(k_{12})^2\lambda_1\lambda_2 \\
&- 16(k_{12})^2\lambda_3^2 - 16(k_{12})^2\lambda_3\lambda_4 - 4(k_{12})^2\lambda_4^2 + 6(k_2)^2\lambda_1\lambda_3 + 12(k_2)^2\lambda_1\lambda_4 \\
&+ 18(k_2)^2\lambda_1\lambda_5 - 36\lambda_1\lambda_2\lambda_3\lambda_c - 72\lambda_1\lambda_2\lambda_4\lambda_c - 108\lambda_1\lambda_2\lambda_5\lambda_c + 48\lambda_3^2\lambda_4\lambda_c \\
&+ 48\lambda_3^2\lambda_5\lambda_c + 16\lambda_3^3\lambda_c + 36\lambda_3\lambda_4^2\lambda_c + 48\lambda_3\lambda_4\lambda_5\lambda_c + 12\lambda_4^2\lambda_5\lambda_c + 8\lambda_4^3\lambda_c\,, \qquad \text{(C.9a)}
\end{aligned}
$$

$$
\begin{aligned}
c_1 =& -6(k_1)^2\lambda_2 - 2(k_1)^2\lambda_3 - 4(k_1)^2\lambda_4 - 6(k_1)^2\lambda_5 + 8k_1k_2\lambda_3 + 4k_1k_2\lambda_4 \\
&- 12(k_{12})^2\lambda_1 - 12(k_{12})^2\lambda_2 - 6(k_2)^2\lambda_1 - 2(k_2)^2\lambda_3 - 4(k_2)^2\lambda_4 - 6(k_2)^2\lambda_5 \\
&+ 9\lambda_1\lambda_2\lambda_3 + 18\lambda_1\lambda_2\lambda_4 + 27\lambda_1\lambda_2\lambda_5 + 36\lambda_1\lambda_2\lambda_c + 12\lambda_1\lambda_3\lambda_c + 24\lambda_1\lambda_4\lambda_c \\
&+ 36\lambda_1\lambda_5\lambda_c + 12\lambda_2\lambda_3\lambda_c + 24\lambda_2\lambda_4\lambda_c + 36\lambda_2\lambda_5\lambda_c - 12\lambda_3^2\lambda_4 - 12\lambda_3^2\lambda_5 - 16\lambda_3^2\lambda_c \\
&- 4\lambda_3^3 - 9\lambda_3\lambda_4^2 - 12\lambda_3\lambda_4\lambda_5 - 16\lambda_3\lambda_4\lambda_c - 3\lambda_4^2\lambda_5 - 4\lambda_4^2\lambda_c - 2\lambda_4^3\,, \qquad \text{(C.9b)}
\end{aligned}
$$

$$
\begin{aligned}
c_2 =& 2(k_1)^2 + 4(k_{12})^2 + 2(k_2)^2 - 9\lambda_1\lambda_2 - 3\lambda_1\lambda_3 - 6\lambda_1\lambda_4 - 9\lambda_1\lambda_5 - 12\lambda_1\lambda_c \\
&- 3\lambda_2\lambda_3 - 6\lambda_2\lambda_4 - 9\lambda_2\lambda_5 - 12\lambda_2\lambda_c + 4\lambda_3^2 + 4\lambda_3\lambda_4 - 4\lambda_3\lambda_c + \lambda_4^2 \\
&- 8\lambda_4\lambda_c - 12\lambda_5\lambda_c\,, \qquad \text{(C.9c)}
\end{aligned}
$$

$$
c_3 = 3\lambda_1 + 3\lambda_2 + \lambda_3 + 2\lambda_4 + 3\lambda_5 + 4\lambda_c\,, \qquad \text{(C.9d)}
$$

$$
c_4 = -1\,. \qquad \text{(C.9e)}
$$

Appendix D

Field and charge rotations

Suppose we start with three fields such that

$$K_\mu = g_A Y_A A_\mu + g_B Y_B B_\mu + g_C Y_C C_\mu \,. \tag{D.1}$$

Our goal now is to check what is the charge Y_Z of a general linear combination of those three fields Z_μ. Lets then supose this linear combination to be:

$$Z_\mu = aA_\mu + bB_\mu + cC_\mu = \begin{pmatrix} a & b & c \end{pmatrix} \begin{pmatrix} A_\mu \\ B_\mu \\ C_\mu \end{pmatrix} , \tag{D.2}$$

with $a^2 + b^2 + c^2 = 1$.

We can now define a orthogonal rotation matrix such that:

$$\begin{pmatrix} Z_\mu \\ Z'_\mu \\ Z''_\mu \end{pmatrix} = O \begin{pmatrix} A_\mu \\ B_\mu \\ C_\mu \end{pmatrix} , O = \begin{pmatrix} a & b & c \\ \times & \times & \times \\ \times & \times & \times \end{pmatrix} . \tag{D.3}$$

Where Z'_μ and Z''_μ are some combinations of the initial fields orthogonal to Z_μ and to each other. We

can now rewrite K_μ as:

$$K_\mu = \begin{pmatrix} g_A Y_A & g_B Y_B & g_B Y_B \end{pmatrix} \begin{pmatrix} A_\mu \\ B_\mu \\ C_\mu \end{pmatrix} \tag{D.4}$$

$$= \begin{pmatrix} g_A Y_A & g_B Y_B & g_B Y_B \end{pmatrix} O^T O \begin{pmatrix} A_\mu \\ B_\mu \\ C_\mu \end{pmatrix} \tag{D.5}$$

$$= \begin{pmatrix} g_Z Y_Z & \times & \times \end{pmatrix} \begin{pmatrix} Z_\mu \\ Z'_\mu \\ Z''_\mu \end{pmatrix} , \tag{D.6}$$

where,

$$g_Z Y_Z = \begin{pmatrix} a g_A & b g_B & c g_C \end{pmatrix} \begin{pmatrix} Y_A \\ Y_B \\ Y_C \end{pmatrix} , \tag{D.7}$$

and thus,

$$Y_Z \propto \begin{pmatrix} a g_A & b g_B & c g_C \end{pmatrix} \begin{pmatrix} Y_A \\ Y_B \\ Y_C \end{pmatrix} . \tag{D.8}$$

We can then conclude that if a field is a combination of the form of Equation (D.2), then its charge takes the form of Equation (D.8). This can be generalised for any number of fields in the theory.